Vienna Doctoral Programme on Water Resource Systems

Doctoral Thesis

# A CONTRIBUTION TO COMPUTATIONALLY EFFICIENT STRUCTURAL RELIABILITY ASSESSMENT

submitted in satisfaction of the requirements for the degree of
Doctor of Science in Civil Engineering
of the Vienna University of Technology, Faculty of Civil Engineering

Dipl.-Ing. Jan Podroužek

Matrikelnummer 0741389

Doctoral Programme on Water Resource Systems
The Centre for Water Resource Systems
Vienna University of Technology
A-1040 Wien, Karlsplatz 13/222, Austria

Gutachter: Prof. Christian Bucher
Vienna University of Technology
Institute of Building Construction and Technology
Karlsplatz 13/222, A-1040 Vienna, Austria

Gutachter: Prof. Dan M. Frangopol
Lehigh University
ATLSS Research Center
117 ATLSS Drive, Bethlehem, PA, 18015 - 4729, USA

Gutachter: Prof. Drahomír Novák
Brno University of Technology
Institute of Structural Mechanics
Veveří 331/95, 602 00 Brno, Czech Republic

Gutachter: Prof. Alfred Strauss
University of Natural Resources and Life Sciences, Vienna
Institute of Structural Engineering
Peter-Jordan-Straße 82, 1190 Wien, Austria

Vienna, February 2014 ..................................

**Content**

**Acknowledgement**

Foremost, the author would first like to acknowledge the financial support of Austrian Science Funds FWF as part of the Doctoral Programme on Water Resource Systems (DK-plus W1219-N22).

Special thanks belong to the thesis supervisor Prof. Christian Bucher for inspiring discussions, patience, encouragement and offering thorough and excellent feedback. The author cannot think of a better supervisor to have. Also, the support of the institute of structural mechanics at the Technical University of Vienna was excellent.

The role of Prof. Alfred Strauss and the IKI institute at the Universität für Bodenkultur Wien is also greatly acknowledged for the possibility of inclusion in several very interesting projects, the review and feedback.

The cooperation with Franz Bamer is also appreciated for the opportunity to test the proposed identification method on realistic structural models and its abstract derivatives.

Numerous field excursions with Michael-Exner Kittridge in the hydrological open air laboratory (HOAL) opened up a new perspective on environmental modeling and geoscientist’s demand on numerical simulations and formed an interesting interdisciplinary cooperation.

Prof. Frangopol and Prof. Novák deserve special recognition for their excellent review and feedback.

Finally, the role of Prof. Günter Blöschl, the Head of the Institute of Hydraulic Engineering and Water Resources Management and the Director of the Centre for Water Resource Systems of the Vienna University of Technology is greatly appreciated for providing the vital skill of disciplined critical thinking.

## 1. Introduction

Since the days of John Von Neumann and Stanislaw Ulam the growth of digital simulations in size and complexity follows the development of processing capabilities of increasingly available computers. Although currently it may seem that a limit of processing speed increase has approached, the trend continues along the cluster computing, i.e. by parallelization of both hardware and solution schemes, e.g. [Foster et al. 2001] or the Vienna Scientific Cluster [Zabloudil 2012].

In such context the following question emerges naturally to both scientists as well as engineers: What is the necessary amount of information to be processed in a model that leads to optimal decisions [Rubinstein 1998]. Although such thinking easily leads to open philosophical questions, such as determinism and the role of chance [e.g. Schaffer 2007], observer's dilemma or selective observation effect [Steineck and Clausius 2013], a contribution based on hard scientific evidence can be made by e.g. studying the phenomena of uncertainties and randomness [Bucher 2009], focusing on particular levels of detailing and by identifying various sources, as conceptually shown at fig. 1. At a certain level, the increase of processed information does not lead to increase of predictive performance.

It could be argued on a valid basis that so defined redundant information can nevertheless be important in order to quantify the estimate of statistical properties of actions based on such prediction, such as safety, risk, probability of failure, robustness, resilience, redundancy, etc. [Der Kiureghian and Liu 1986, Frangopol and Curley 1987]. However, the extent of universality of such argument is also limited, since it is believed by the author and partially proven in the presented thesis that an unprofitable component of randomness always exists such that it is redundant in any frame of reference, including the conceptually most correct full probabilistic assessment [Ang and Tang 2007].

Somewhat naturally, simulation tasks are commonly formulated such that the scope of information to be processed is far beyond the currently available computational capacity. Despite rapid advancements in computational availability and capacity, the unsatisfiable demands from the modeling and simulation community drives the spiral loop of processing power increase and the necessity of adopting model and Monte

Carlo (MC) -type simulation reduction schemes [Kahn, 1949, Kahn and Marschall, 1953].

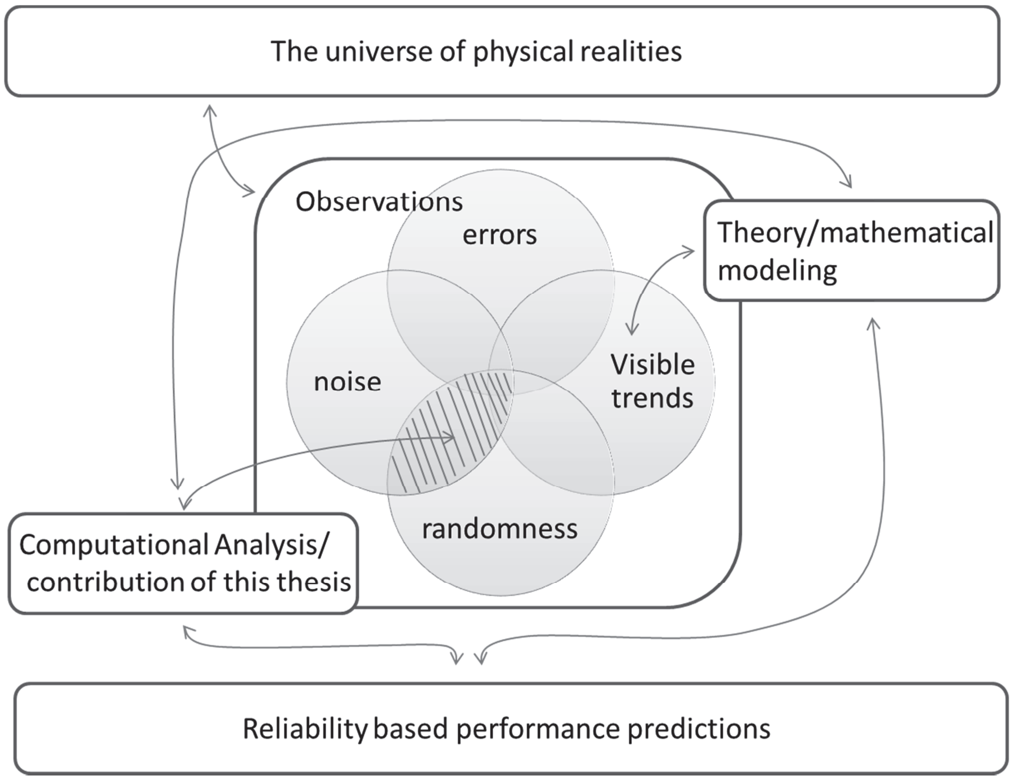


*Fig. 1. Various observers' perspective on the components of uncertainty and the complementary role of computational analysis of randomness and classical mathematical theory.*

Model (order) reduction techniques [Bamer and Bucher 2012] and the MC task reduction schemes can be considered as supertemporal and their application does not create a demand for further reduction, unlike the case of accelerated hardware performance. Among the scientific community, special sampling design and model reduction methods are increasingly popular as they still hold a potential of numerous major breakthroughs and simply because the scope of computational universe goes beyond the laws of currently accepted physics, a universe full of abstractions free for all, given the availability of computers and imagination.

In the following chapters the author will elaborate these arguments in the context of civil engineering systems subjected to ever changing environment. The necessity of quantifying the performance of such systems on a probabilistic basis reveals the full potential of the following considerations. Following text presents 3 already published papers and an annex describing the essential code for reproducibility of the research as published in chapter 2 and 3. The author of this thesis wishes the readers an undisturbed experience and comprehensive view on the subject of probability based performance assessment of structural systems and infrastructure, with the focus on natural phenomena.

In chapter 2 the discussion concerns environmental loads that need to be considered as time-varying stochastic phenomena acting on engineering infrastructure. The objective is to evaluate such actions in a probabilistic context. It is further assumed that due to nonlinear effects in infrastructure models and temporal representation of probabilistically different events [Deodatis 1996], closed-form solutions do not exist and common approximation methods fail, i.e. Monte Carlo type of assessment is required in order to solve the limit state functions. As this is computationally unfeasible, reduction schemes are commonly sought on both model and load representation side as well as on number of repeated trials. In the particular case presented, i.e. seismic protection, the high dimensional MC problem is reduced by introducing a novel method that enables an effective pre-screen of MC samples, or in the presented case, the identification of critical ground motion records with respect to given mechanical oscillators. Determination of various threshold exceedance probabilities served for benchmarking against the reference brute-force MC method, arithmetic mean and randomly sampled realizations at the same cost of the proposed reduction method. The comparison revealed that critical samples can be identified at a fraction of the reference cost (1,5%) and served as motivation for further research in the subject of importance sampling for dynamical systems.

Chapter 3 further focuses on the utilization of image processing and pattern recognition techniques towards the goal as described in chapter 2. It reveals, among others, that for few process-model scenarios, the importance classification rules can be based on visual comparison of graphical representation of the original set of stochastic processes (e.g. according to [Priestley, 1965]). This evidence has led to a hypotheses that pattern recognition techniques could be trained to solve the identification problem. Due to only partial success in solving the test cases, the approach diverged to more general formulation, which later become designated as STS. It still utilizes graphical representation of the time-series, adding stochastic sensitivity analysis of a small training sample set and consistently identifies the critical processes, including the non-stationary and non-separable types of artificially generated ground motion records acting upon non-linear mechanical oscillators with arbitrary degrees of freedom. The presented results implies a new importance sampling strategy for structural transient formulations and analogous problems in environmental sciences, e.g. in water resources context precipitation scenarios for hydrological routing models.

The following chapter 4 attempts to capture „all possible“ deterioration states, unlike the uniform class of stochastic processes from previous chapter, in order to quantify resistance of a particular engineering infrastructure against events unaccounted for during design phase and/or unexpected during operation. It is worthwhile to note here that the „all possible“ term denotes a possibilistic approach (e.g. [Marano and Quaranta 2010]) rather than probabilistic one, hence it is difficult, if impossible, to assign probabilities to unexpected or rare events, which cannot be described by a scalar value or function, like in the case of e.g. return periods in hydrology, where theoretical distribution functions are more less effectively used to model flow quantitates. Existing prestressed box-girder bridge serves as a demonstration example where the consequences of environmental loads, uncertainty and random nature are combined and evaluated. Here various damage scenarios were explicitly modeled using the available information on bridge condition from past inspections. Finally, such artificially generated realizations were computed as detailed 3D Non-linear models on a fully probabilistic basis [Cervenka 2013], taking into account know distributions of material properties, prestressing forces and geometrical imperfections. Argument behind such an attempt is the number of emerging performance damage-based indicators, such as robustness, redundancy or resiliency, requiring higher-order variable statistics [Biondini and Frangopol 2012]. Typically, the problem is treated on a component-removal level, however, isostatic systems, like the presented bridge, receives very little attention. The uniqueness of this chapter is therefore mainly in adopting the damage-based performance indicators for isostatic systems, where straightforward removal of discrete components is not possible.

*Chapter 2: Research paper published in Structural Safety Journal*

**Identification of critical samples of stochastic processes towards feasible structural reliability applications**

Jan Podrouzek, Christian Bucher, George Deodatis

http://dx.doi.org/10.1016/j.strusafe.2013.10.005

Publication History
Accepted manuscript online: 26 NOV 2013
Manuscript Accepted: 21 OCT 2013
Manuscript Revised: 21 OCT 2013
Manuscript Received: 11 FEB 2012

Editor-in-Chief: B. R. Ellingwood (USA)
5-Year Impact Factor: 2.382

Online ISSN: 0167-4730

Structural Safety (2013)

Contents lists available at ScienceDirect

Structural Safety

journal homepage: www.elsevier.com/locate/strusafe

# Identification of critical samples of stochastic processes towards feasible structural reliability applications

Jan Podrouzek[a,*], Christian Bucher[b], George Deodatis[c]

[a]The Centre for Water Resource Systems, Vienna University of Technology, A-1040 Wien, Karlsplatz 13/222, Austria
[b]Institute of Building Construction and Technology, Vienna University of Technology, A-1040 Wien, Karlsplatz 13/222, Austria
[c]Santiago and Robertina Calatrava Family Professor, The Fu Foundation School of Engineering and Applied Science, Columbia University, 630 SW Mudd, Mail Code: 4709, New York, NY 10025, USA

ARTICLE INFO

*Article history:*
Received 11 February 2012
Received in revised form 21 October 2013
Accepted 21 October 2013

*Keywords:*
Stochastic process
Critical excitation
Reliability analysis
Importance sampling
Image processing
Pattern recognition
Identification problem

ABSTRACT

This paper contributes to the structural reliability problem by presenting a novel approach that enables for identification of stochastic oscillatory processes as a critical input for given mechanical models. The proposed method is based on a graphical representation of such processes utilizing state of the art image processing and pattern recognition techniques, leading to a set of finite rules that consistently identifies those realizations of stochastic processes that would lead to a critical response of a given mechanical model. To examine the validity of the suggested method, large sets of realizations of artificial non-stationary processes were generated from known models, several criteria for critical response were formulated and the results were statistically evaluated. The promising results suggest important applications that would dramatically decrease computational costs e.g. in the field of probabilistic seismic design. Further examination may lead to a formulation of a new class of importance sampling techniques.



## 1. Introduction

The necessity for adopting fully probabilistic design concepts has become imperative when considering static loads [1,2]. On the other hand, structural dynamics is still far from a practical utilization of such concepts despite cheap contemporary computational costs. This is mainly due to the uncertain nature of environmental loadings that have to be modeled as time-varying phenomena, represented in this paper by non-stationary stochastic oscillatory process as defined by Priestley [3].

It is a well-accepted fact that structures respond in a very uncertain manner to probabilistically different ground motion events while there is very limited a priori knowledge on the structural behavior. An implication is the necessity to perform the structural analysis for each realization of the event separately, which makes the Monte-Carlo based reliability analysis computationally unfeasible for some realistic assumptions, i.e. small probabilities and large sample sizes.

There have been several recent attempts to avoid such reliability problems in their full form. Moustafa [4] proposed a framework for deriving optimal earthquake loads expressed as a Fourier series. More recently, critical excitation methodologists propose to identify critical frequency content of ground motions maximizing the mean earthquake energy input rate to structures (for details see e.g. [5]). From a different perspective, Barbato et al. [6] approximate the first passage problem by formulating exact closed form solutions for the spectral characteristics of random processes. Macke et al. [7] present an importance sampling technique for randomly excited dynamical systems.

Authors of this paper attempt to maintain the up-to-date conceptually correct fully probabilistic concept [8] while reducing the number of required analyses by means of the proposed identification framework. It is based on a non-traditional assumption that there exists a finite set of rules capable of classifying synthetic samples of stochastic processes according to their importance as a critical input for a given mechanical model. Whether such sets of rules could be formulated for an arbitrary system remains an open problem for further research.

## 2. Development

The identification strategy follows a transparent image processing paradigm completely independent of structural dynamics, thus representing a nontraditional option in the field. The reason behind such argument is experimental, aiming at delivering a simple and wide-purpose method.

The main objective can be formulated as follows: find the critical realization of a stochastic process from a target sample set $\boldsymbol{S}$ under defined critical response criteria. In the following text the symbol $\rightarrow$ designates higher order mapping function, e.g. $x_0 \rightarrow f(x_0)$.

Suggested Small Training Set (STS) input format:

* Corresponding author. Tel.: +43 1 58801 22301.
*E-mail address:* podrouzek@waterresources.at (J. Podrouzek).

0167-4730/$ - see front matter © 2013 Published by Elsevier Ltd.
http://dx.doi.org/10.1016/j.strusafe.2013.10.005

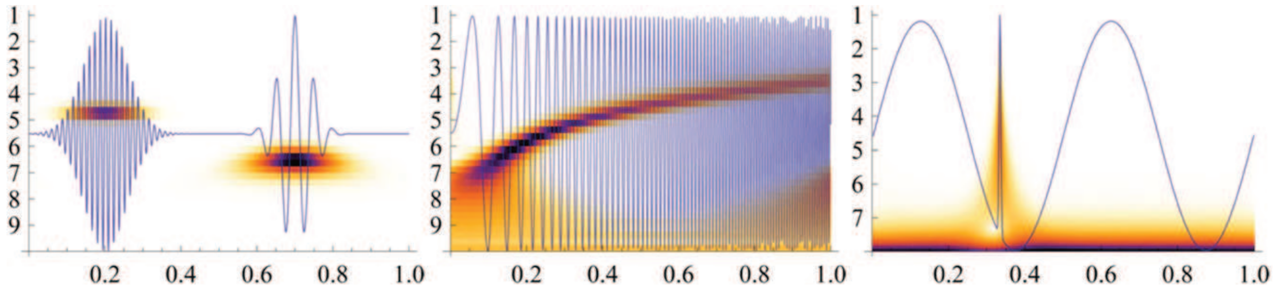


**Fig. 1.** Relationship between the signal and the ***G*** pattern. Horizontal axes represents time and is joined for both the signal and ***G***. Vertical axis of ***G*** represents the equivalent scales (octaves or frequency bands).

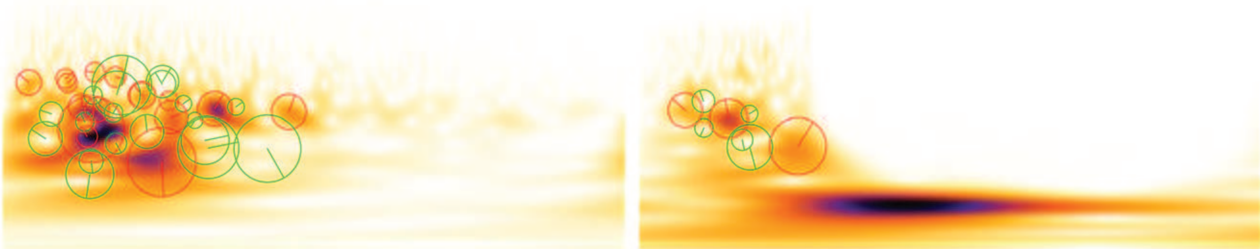

**Fig. 2.** Graphical representation (***G***) of L1 (left) and L2 (right) in the form of Wavelet Scalogram and visualized detected keypoints (***R***) described by radius, orientation and contrast sign (circle, rotation and color). (For interpretation of the references to colour in this figure legend, the reader is referred to the web version of this article.)

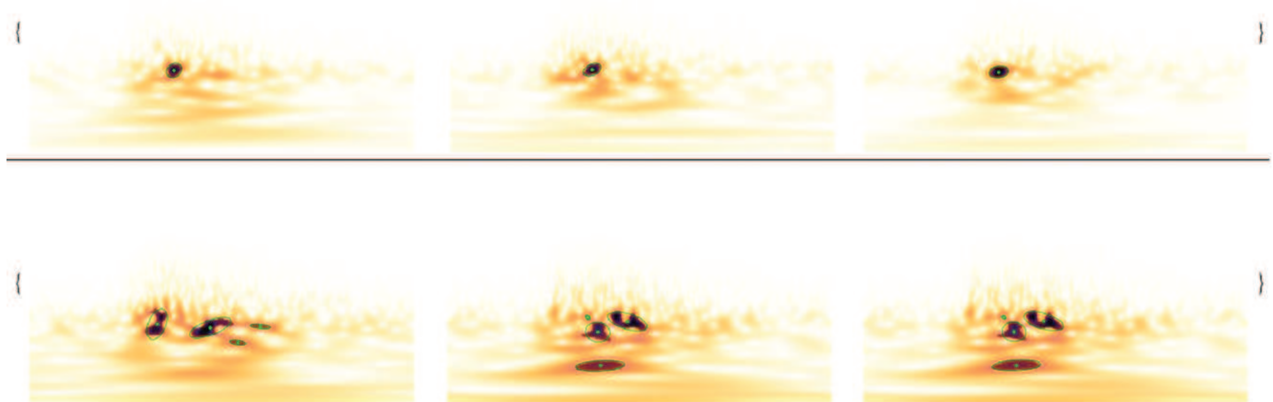

**Fig. 3.** Number of fitted oriented ellipses (based on SURF) as a performance indicator. Upper row: 3 ranked maximum and lower row: 3 ranked minimum responses.

(i1) Finite set ***S*** of 1-dimensional stochastic process realizations $\boldsymbol{r_i}$

$$\boldsymbol{r_i} \in \langle v_1, v_2, \ldots, v_t \rangle \tag{1}$$

$$\boldsymbol{S} \in \langle \boldsymbol{r_1}, \boldsymbol{r_2}, \ldots, \boldsymbol{r_n} \rangle \tag{2}$$

where $v_i$ can be an arbitrary value, e.g. acceleration values recorded in $t$ time steps. The notation $n$ is used for the size of ***S***.

(i2) Arbitrary deterministic solver, typically extremely expensive computational numerical integration, e.g. FEM, or reduced meta-models such as MOR and POD [9],

$$F(\boldsymbol{r_i}) \overset{N\,Solve}{\rightarrow} y_i \tag{3}$$

returning an arbitrary scalar response quantity $y_i$, e.g. a peak displacement.

(i3) Arbitrary algorithm for 2-dimensional graphical representation ***G*** of $r_i$. Among the two general options maintaining the physicality of the ***G*** product is the evolutionary spectra [10] or the wavelet–vector coefficients based scalogram [11] *wd*. The latter is used in this paper due to preferable computational complexity, basic principles demonstrates sample patterns at Figs. 1 and 2.

$$wd(\boldsymbol{r_i}) \overset{maps}{\rightarrow} \boldsymbol{G_i} = \begin{bmatrix} c_{1,1}^{(i)} & \cdots & c_{t,1}^{(i)} \\ \vdots & \ddots & \vdots \\ c_{1,o}^{(i)} & \cdots & c_{t,o}^{(i)} \end{bmatrix} \tag{4}$$

Here the wavelet vector coefficients (1,. . .,$o$) are plotted as rows of colorized rectangles $c_{t,o}$, in which large absolute values are shown darker and each subsequent row corresponds to different wavelet index specifications. Note that the actual choice of the mapping algorithm in this step is quite immaterial for proper functioning of the method as long as it allows a time-frequency decomposition of the signal.

(i4) Parameters vector and admissible intervals $f\langle 1 \ldots (t \times o) \rangle$, $m\langle 1 \ldots n \rangle$, $p\langle 1 \ldots m/2 \rangle$, $q\langle 1 \ldots m \rangle$

Proposed STS strategy steps:

(s1) Construct a training subset ***s*** randomly sampled from ***S*** having the length $m \ll n$.

$$\boldsymbol{s} \in \langle r_1, r_2, \ldots, r_m \rangle \tag{5}$$

(s2) Solve the training subset $\boldsymbol{s}$:

$$(r_1), F(r_2), \cdots, F(r_m)\rangle \overset{yields}{\rightarrow} \boldsymbol{s_F} \in \langle y_1, y_2, \cdots, y_m \rangle \tag{6}$$

(s3) Create ranked minimum and maximum sets $\boldsymbol{S_{F,min}}$ and $\boldsymbol{S_{F,max}}$:

$$\boldsymbol{s_{F,\mathrm{min}}} = \langle 1, \ldots, p \rangle^{th} \text{ smallest elements in } \boldsymbol{s_F} \tag{7}$$

$$\boldsymbol{s_{F,\mathrm{max}}} = \langle 1, \ldots, p \rangle^{th} \text{ largest elements in } \boldsymbol{s_F} \tag{8}$$

(s4) Transform $\boldsymbol{r_i}$'s corresponding to $\boldsymbol{S_{F,min}}$ and $\boldsymbol{S_{F,max}}$ into graphical representation

$$wd(\boldsymbol{r_{s_{F,\mathrm{min}}}}), wd(\boldsymbol{r_{s_{F,\mathrm{max}}}}) \overset{yields}{\rightarrow} \langle \boldsymbol{G}_{\mathbf{min},1}, \ldots, \boldsymbol{G}_{\mathbf{min},\boldsymbol{p}} \rangle, \langle \boldsymbol{G}_{\mathbf{max},1}, \ldots, \boldsymbol{G}_{\mathbf{max},\boldsymbol{p}} \rangle \tag{9}$$

(s5) Find a finite set of rules $\boldsymbol{R}$ such that consistently maps the s4) products to the corresponding few important (i.e. maximal or critical) response criteria. Note that a one-to-one correspondence is likely unfeasible and the search domain can be effectively narrowed by ignoring the pixels with constant or random behavior. A simple specific form of $\boldsymbol{R}$ can be attained by calculating the 2-dimensional correlation pattern $\boldsymbol{P}$ using the $\boldsymbol{G_{min}}$ and $\boldsymbol{G_{max}}$:

$$\boldsymbol{P} = \left| \sum_{i=1}^{p}\sum_{x=1}^{t}\sum_{y=1}^{o} \frac{c_{x,y}^{(\mathrm{min},i)}}{p} - \sum_{i=1}^{p}\sum_{x=1}^{t}\sum_{y=1}^{o} - \frac{c_{x,y}^{(\mathrm{max},i)}}{p} \right| \tag{10}$$

From the formula above it is clear that $\boldsymbol{P}$ has the same dimension as $\boldsymbol{G}$ and that the higher values $\boldsymbol{P}$ coefficients hold, the more relevant this location became for the classification of the original set $\boldsymbol{S}$ (for a sample pattern see Fig. 4 left). Another form of correlation structure ($\boldsymbol{R}$) can be i.e. the number of fitted oriented ellipses (see Fig. 3), however applicability of such rule is very limited and therefore is demonstrated here only as a rare instance when visual features themselves enable for classification of $\boldsymbol{S}$. In the following text a concrete form of $\boldsymbol{R}$, i.e. $\boldsymbol{P}$, will be used to help the reproducibility of the STS strategy.

(s6) Quantification of important Features $\boldsymbol{QF_i}$ on the original set $\boldsymbol{S}$ using the summation of $j$th largest element in $P$ (denoted as $P_{le}(j)$) multiplied by $\boldsymbol{G_i}$ element at corresponding position of $j$th largest element in $P$ in terms of $t,o$ indices, denoted as $G_{cp}(i,j)$ projection.

$$\boldsymbol{S} \overset{wd(\boldsymbol{ri})}{\rightarrow} \boldsymbol{G_S} \tag{11}$$

$$\boldsymbol{QF_S} \left\langle \sum_{j=1}^{f} P_{le}(j) \times G_{cp}(1,j), \sum_{j=1}^{f} P_{le}(j) \times G_{cp}(2,j), \ldots, \sum_{j=1}^{f} P_{le}(j) \times G_{cp}(n,j) \right\rangle \tag{12}$$

(s7) Classification of $\boldsymbol{S}$ according to the highest values of $\boldsymbol{QF_s}$ with respect to the response quantity $y_i$. Both values $\boldsymbol{QF_i}$ and $y_i$ are correlated now and the identification results are known. The associated likelihoods can be approached as evidence supporting the hypotheses $y_i \geq {}_{max}$:

$$\text{Probability}\,(y_i \geq y_{\mathrm{max}}) = \frac{1}{n} \tag{13}$$

In the broader context one should consider the STS strategy as a fast MC samples pre-screen to limit the number of necessary executions of numerical analysis of the mechanical model. It is assumed that mechanisms behind rules extracted from reasonably small samples are applicable to arbitrarily larger sample. Clearly, whenever using a black-box type of approach, there is a risk of extracting mechanisms that apply only to the training sample if its sample size is too small or in cases of "statistical bad luck". The determination of minimal size of a training set should be based on a requirement for STS's predictive confidence, quantified by a proposed performance index as part of the STS. It should be noted, however, that the confidence intervals for various process–model combinations have to be defined individually (e.g. note various vertical scales in Fig. 11).

In the following text graphical representation of the particular ground motion time history has the form of Gabor Wavelet Scalogram, visualization at Fig. 1 highlights the basic concept. First example resolves time and frequency features (20 and 70 Hz) of a signal, second shows sinusoid with linearly increasing frequency and the last example demonstrates good time localization of a feature $\mathrm{Sin}[4\pi t] + 2\mathrm{Exp}[-10^5(1/3 - t)^2]$. More on the evolutionary behavior of spectral characteristics utilizing wavelet coefficients can be found e.g. in the dissertation of Tezcan [12] including explicit relationship between the harmonic wavelet coefficients of a process and its time dependent spectral content.

As stated before, the proposed STS strategy aims at general and automated feature extraction. It should be noted here, however, that in rare instances visual comparison of the ranked scalograms $\boldsymbol{G}$ itself enabled the formulation of the identification rule $\boldsymbol{R}$ by comparing the number of regions with steep contrast gradient, i.e. image keypoints (Fig. 2). For such feature, a number of standardized algorithms exists, e.g. implemented Speeded Up Robust Features (SURF, [13]), a scale- and rotation-invariant interest point detector and descriptor. Such an approach can be interpreted as assessment of localization of energy in the time domain and proved to be consistent for configurations of SDOF oscillators excited by stationary or amplitude modulated processes. In such instances, a low number of detected keypoints indicates a critical process, i.e. $\boldsymbol{G}$ has minimal scatter of excitation energy as seen in Fig. 3.

The most general version of STS utilizes $f$ few pixels of a small-resolution Wavelet Scalogram image $\boldsymbol{G}$ and correlation pattern $\boldsymbol{P}$. Ideally, the values of particular $\boldsymbol{G_i}$ pixels localized by the most sensitive $\boldsymbol{P}$ pixels vary systematically according to the ranked small sample training sets as can be seen in Fig. 4. If not, the correlation can be optimized by adjusting the p and f parameters without increasing the number of expensive $F(\boldsymbol{r_i})$ computations.

The sensitive pixels typically form clusters, in some instances a line indicating a dominant frequency band (Fig. 4). Regardless of the attractiveness of emerging questions on the physical connections of these clusters to the mechanical models (and dominant frequencies), such debates will not be detailed here due to the limited scope of the paper. For a related discussion see the work of e.g. Drenick [14].

## 3. Design point motivating pattern

The choice of wavelet coefficients as indicators of relevant excitation patterns will be motivated by a simple example. For a linear single-degree-of-freedom system subjected to white noise $w(t)$ excitation it is well known that the most likely excitation pattern leading to first passage of a displacement threshold at a given time $t$ is given in terms of the time-reversed impulse response function [15,16]. For an oscillator described by the equation of motion

$$\ddot{x} + 2\zeta\omega\dot{x} + \omega^2 x = w(t) \tag{14}$$

in which $\zeta = 0.05$, $\omega = 3$ the design point excitation for time $T = 20$ s is shown in Fig. 5.

**Fig. 4.** Correlation pattern on the left: Array of pixels (rescaled) according to their behavior, the darker the color, the more sensitive the pixel is to the ranked $G_s$, while lighter colors indicate random or invariant behavior. Right: corresponding position of these pixels on the wavelet scalogram of particular realization.

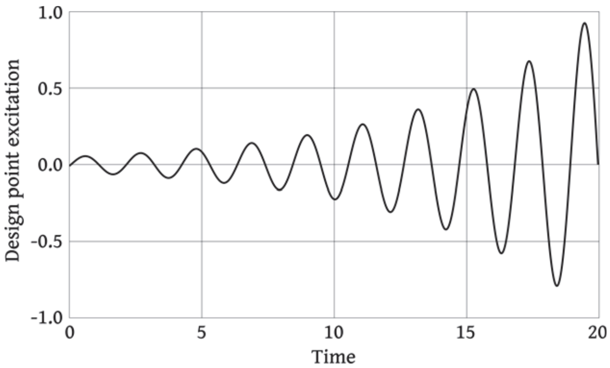


**Fig. 5.** Design point excitation for linear SDOF oscillator subject to stationary white noise.

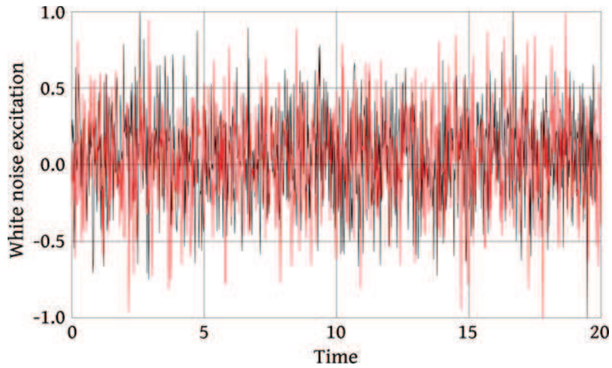


**Fig. 7.** White noise sample functions.

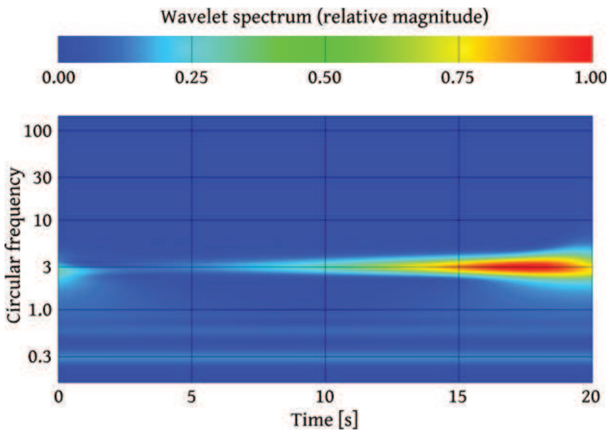


**Fig. 6.** Gabor wavelet transform of design point excitation.

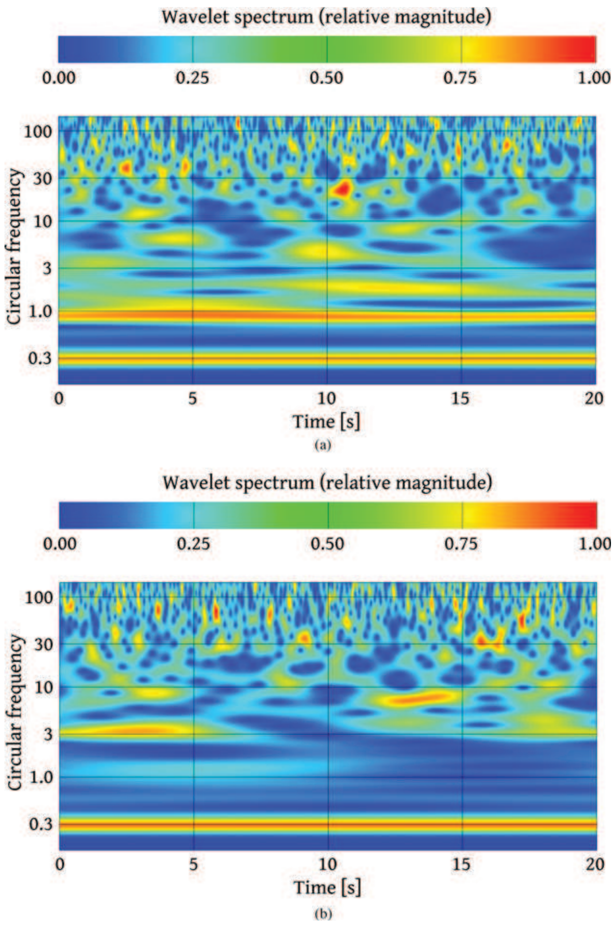


**Fig. 8.** Gabor wavelet transform of white noise sample functions.

The Gabor wavelet transform of this design point excitations is shown in Fig. 6. This figure clearly shows the increasing intensity in the frequency range around 3 rad/s (which matches the natural circular frequency of the oscillator) towards the end of the time interval.

In contrast, actual realizations of white noise as shown in Fig. 7 do not exhibit any immediately recognizable time–frequency patterns. For the two samples as shown in Fig. 7, the Gabor wavelet transforms are shown in Fig. 8.

In order to recognize a pattern in the random arrangement in time–frequency, the correlation between the oscillator response $x$ at time $T$ and the individual wavelet coefficients (pixel) is computed. This computation is based on 1000 realizations of the white noise. The coefficient of correlation is then plotted in the same arrangement as the wavelet coefficients. This is shown in Fig. 9. This correlation pattern exhibits a remarkable similarity to the wavelet transform of the design point excitation. It is therefore obvious that for each

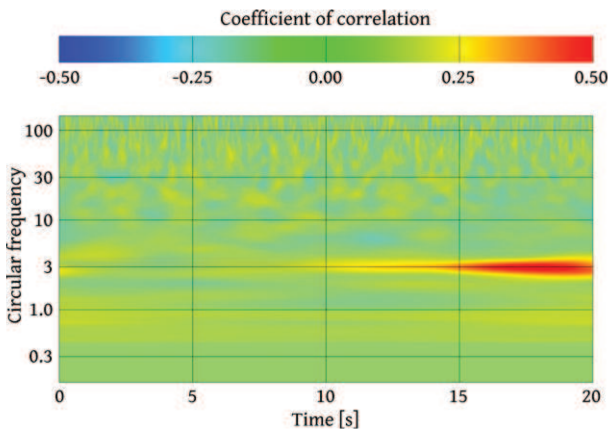


**Fig. 9.** Design point equivalent correlation pattern between wavelet coefficients and oscillator response $x(T)$.

sample function of the white noise, the degree of similarity between this correlation pattern and the actual wavelet transform gives an indicator of relevance. Such an indicator (***QF***) can easily be computed in this motivating example by a normalized projection of the wavelet transforms on the identified correlation pattern.

The presented evidence validates the implementation towards identification of critical samples of realistic excitation patterns coupled with various structural models and consequent importance sampling.

## 4. Acceleration and structural models

For the validation of the STS method four distinct combinations of two models (M1 and M2) and two loadings (L1 and L2) are considered. The mechanical models represent a single degree of freedom (SDOF) damped linear oscillator (M1) and a nonlinear seismically isolated SDOF on a friction pendulum system (M2) subjected to an earthquake loading $F(t) = -ma(t)$. Here $m$ is the mass of the SDOF system and $a(t)$ is the ground acceleration described as (L1) an amplitude modulated random process

$$a(t) = e(t) \cdot b(t) \tag{15}$$

where $e(t)$ is the amplitude modulating function (see rescaled plot as dashed line in Fig. 10) given by

$$e(t) = 4\left[\exp(-0.25t) - \exp(-0.5t)\right] \qquad \text{for } t > 0 \tag{16}$$

and $b(t)$ denotes a stationary zero-mean Gaussian random process (Kanai-Tajimi filter [17]) with power spectral density

$$S_{bb}(\omega) = S_0 \left[ \frac{1 + 4\zeta_g^2 \left[\frac{\omega}{\omega_g}\right]^2}{\left\{1 - \left[\frac{\omega}{\omega_g}\right]^2\right\}^2 + 4\zeta_g^2 \left[\frac{\omega}{\omega_g}\right]^2} \right] \tag{17}$$

The second ground acceleration model (L2), is amplitude and frequency modulated random process whose objective is to reproduce the general frequency variation characteristics of an acceleration record from the 1964 Niigata earthquake described by the Bogdanhoff–Goldberg–Bernard (1961) envelope function

$$A(t) = a1\ t \exp(-a2\ t) \qquad \text{for } t > 0 \tag{18}$$

and the Clough–Penzien [17] correction to the Kanai–Tajimi acceleration spectrum with parameters $S_0$, $\omega_g$ and $\zeta_g = \zeta_f$ as functions of

**Table 1**
Mechanical models and structural data.

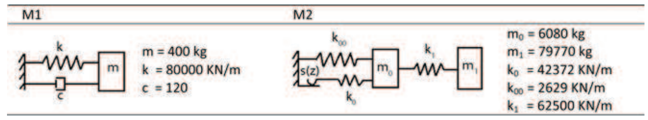


time:

$$\begin{aligned} S(\omega, t) = S_0(t) &\left[ \frac{1 + 4\zeta_g^2(t)\left[\frac{\omega}{\omega g(t)}\right]^2}{\left\{1 - \left[\frac{\omega}{\omega g(t)}\right]^2\right\}^2 + 4\zeta_g^2(t)\left[\frac{\omega}{\omega g(t)}\right]^2} \right] \\ &\times \left[ \frac{\left[\frac{\omega}{0.1\omega g(t)}\right]^2}{\left\{1 - \left[\frac{\omega}{0.1\omega g(t)}\right]^2\right\}^2 + 4\zeta_f^2(t)\left[\frac{\omega}{0.1\omega g(t)}\right]^2} \right] \end{aligned} \tag{19}$$

$$S_0(t) = \frac{\sigma^2}{\pi\, \omega_g(t)\left(2\zeta_g(t) + \frac{1}{2\zeta_g(t)}\right)} \tag{20}$$

$$\omega_g(t) = \begin{cases} 15.56, \ 0 \le t\&4.5 \\ 27.12(t-4.5)^3 - 40.68(t-4.5)^2 + 15.56, \ 4.5 \le t\&5.5 \\ 2.0, \quad t \ge 5.5 \end{cases} \tag{21}$$

$$\zeta_g(t) = \begin{cases} 0.64, \quad 0 \le t\&4.5 \\ 1.25(t-4.5)^3 - 1.875(t-4.5)^2 + 0.64, \quad 4.5 \le t\&5.5 \\ 0.015, \ t \ge 5.5 \end{cases} \tag{22}$$

where parameters $a_1 = 0.68$, $a_2 = 0.25$ and $\sigma = 100$. Eqs. (21) and (22) represent a soil liquefaction model proposed by Deodatis and Shinozuka [18]. Simulation techniques for stationary and non-stationary processes were adopted from [19,20], respectively.

The nonlinear mechanical model M2 represents a SDOF system combined with a friction based seismic isolation device (friction pendulum system) that introduces another mechanical degree of freedom as well as an internal variable representing plastic slip $z$. This model was adopted from [21] and will not be detailed in this paper. The structural data for both M1 and M2 are provided in Table 1, while random realizations (sample functions) of L1 and L2 and the corresponding responses are depicted in Fig. 10.

The critical response criterion has been formulated either as the absolute value of the maximum displacement of the mass most distant from the application of the seismic load or as a given percentile of the mean-square value of the response displacements. The former criterion leads to better identification performance $Ip$ (Eq. (23)), i.e. systematic features are reproduced more efficiently; and therefore is adopted in this paper.

## 5. Identification results

Development and testing of the proposed STS on multiple scales and process–model combinations showed that it is difficult, perhaps impossible, to formulate a general identification rule of physical interpretability. One of these attempts led to the formulation of ***R*** incorporating the image keypoints as a way of quantifying the energy scatter in the loading process.

Consequently, soft computing techniques were used in search of a general black-box type method. The proposed version of STS was tested on a large number of clusters composed from a total of $4.2 \times 10^4$ realizations of the L1 and L2 processes in combination with mechanical models M1 and M2. The stochastic simulations verified the consistency of identified ***R*** for every one of the tested

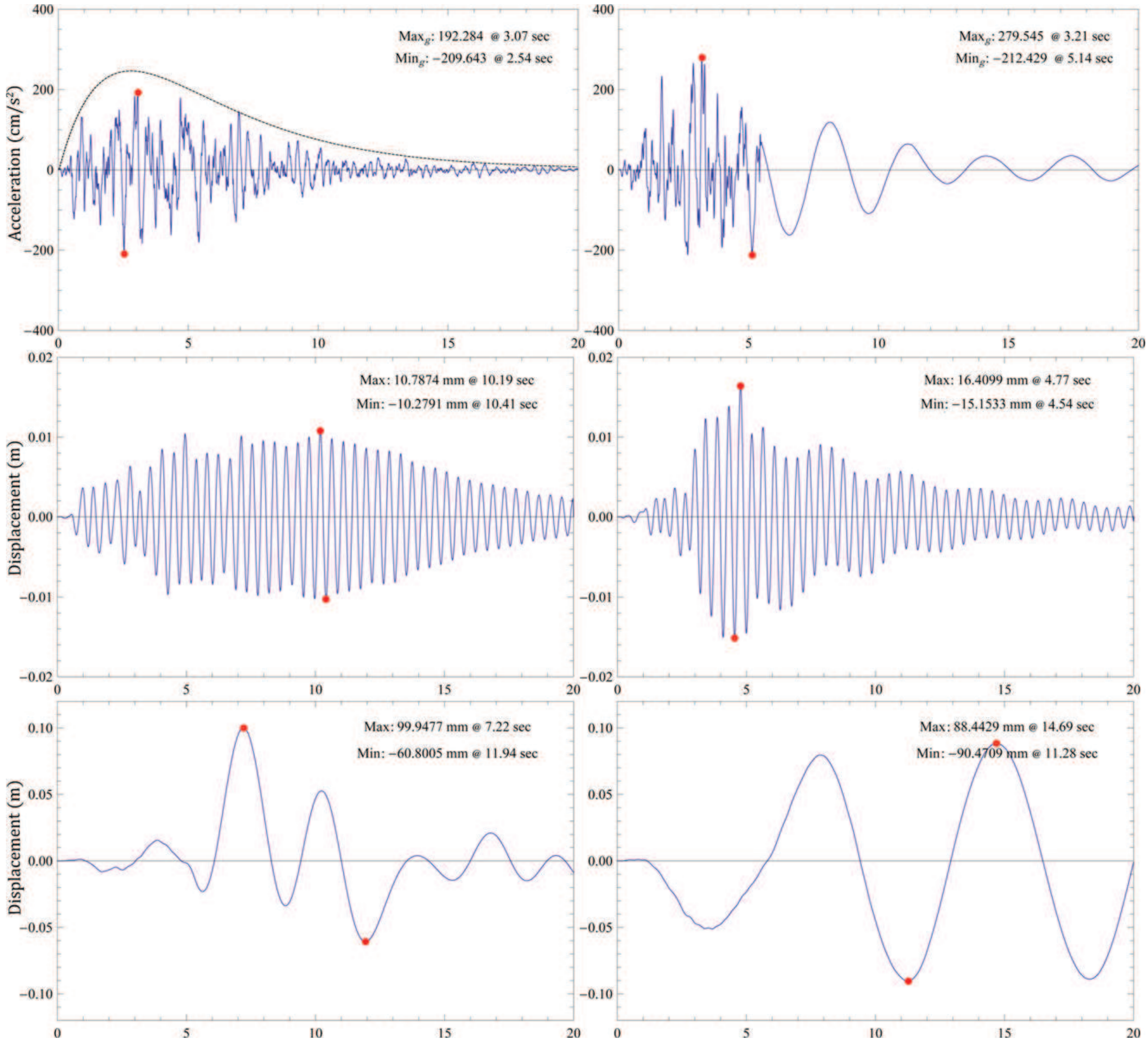


**Fig. 10.** Sample realizations: left column top down: sample of L1 process, M1 and M2 responses to L1; right column top down: sample of L2 process, M1 and M2 responses to L2; time (s) at horizontal axes.

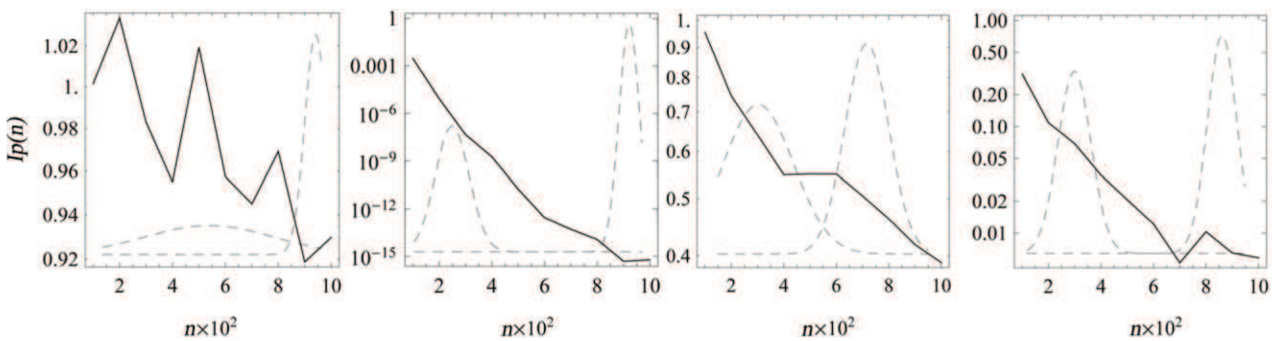


**Fig. 11.** Performance index $Ip$ as a function of sample size $n$ (left to right: L1M1, L1M2, L2M1, L2M2). Dashed lines represent the Normal distribution PDFs fitted to 21 joined min and max sets for sample size $n = 2.1 \times 10^4$. Note the PDFs separation effect on the performance index (different vertical scales).

process-model combinations (persistent trend after resampling). Results presented in Fig. 11 were chosen to demonstrate the variability of performance and do not represent the best or the worst process–model combinations considered.

The performance index *Ip* is defined according to the following integral expression:

$$I_p = \int_0^1 PDF_{\min}(x) PDF_{\max}(x)\, dx \tag{23}$$

where $PDF_{min/max}(x)$ stands for the probability distribution function fitted to $\boldsymbol{QF_S}$ scalar vector (development step s6). Growing separation of these distribution functions corresponds to better performance (see Fig. 12), indicated by the decreasing value of *iP* in Eq. (23). The integration range corresponds to the admissible values of the *G* pixels.

## 6. Sample selection

Following the successful formulation and validation of $\boldsymbol{R}$ according to the proposed STS, the importance sampling strategy is based on applying $\boldsymbol{R}$ to various sizes of $\boldsymbol{S}$ while sorting the stochastic process realizations $r_i$ according to $\boldsymbol{QF_i}$. Then, for each $\boldsymbol{S}$ size the first $q$ corresponding realizations are determined as critical input for the mechanical model. The determination of $q$ depends on the required confidence of the STS strategy, e.g. in the L1M2 model-process combination, $q = 10$, i.e. 1% of the full set (1000). Refer to the right hand side plot of Fig. 13.

The importance sampling test scenario, as described above, proved to be a consistent measure for reducing the 1000 sample set to a smaller size while maintaining the same critical response characteristics. The STS utilized a 100 sample training set (10%) and the consequent importance sampling required an additional 10 analyses (1%), therefore reducing the computational task by 89%. The additional 1% ensured that the important sample (most critical response) was captured by over 91% (within 21 test runs).

It should be noted here that optimal *f* parameter follows from the inverse U-shaped curve logic, i.e. neither high nor low *f* values are desirable. This is demonstrated by the presented example from Fig. 14 where $f = 1$. Here note the effect of an emergent 2nd branch STS artifact from the *y* distribution plot according to the ranked *QF*. The inverse of the same plot (Fig. 13) does not exhibit such effect, representing the amount of unaccounted information by STS mainly due to incorporating only a single dominant pixel to reproduce the systematic behavior of a several clusters of sensitive pixels. With increasing *f* the *QF* benefits from utilizing the sum of *f-most* sensitive pixels (Eq. (12)) until a point where many less sensitive pixels outweigh the few important and the identification results start following the RND curve of Fig. 15. The presented *QF* quantification can be further improved assigning weighs to each subsequent *f* value or by including the directional effects of $\boldsymbol{P}$, following e.g. the spatial changes of the steepest contrast gradient.

Choosing the graphical domain as part of the STS strategy delivers clear benefits in terms of transparency, efficiency and robustness; however, there is also a problematic aspect arising from the ambiguous low color depth RGB channels. This effect can be observed in Fig. 14 as the top horizontal row of *y* points. Ideally, all such points should concentrate around the coordinate [0, 1]; however, as the critical response is represented by a scalar maximum, it is sufficient to capture any instance of such scalar maxima and therefore such aspect can be tolerated. In either case, uniqueness of the QF labels (currently RGB values of sensitive pixels) can be easily ensured by e.g. enhancing the RGB values with random binary sequences of given length.

The effect of unaccounted information does not only exhibit itself via the 2nd branch, but clearly also by the inability to always capture the single *y* maximum, as one might observe on the comparison plot in Fig. 15. Here the goal is to determine the probability of exceeding a critical displacement threshold $u_{lim}$ at different sample size scales and compare it against reference pure Monte Carlo (MC) values.

In terms of accuracy, the maximum reached deviation between the MC reference and STS value was 7.8%. However, in terms of computational efficiency, the STS based importance sampling utilized only a fraction of the MC computational cost, e.g. 1.5% for the $10^4$ sample size ($m = 1\%$ of $n$ and $q = 50\%$ of $m$). Due to its substantial computational advantage, however, the present approach will be suitable especially for reliability-based design optimization problems for which the reliability analysis has to be repeated frequently.

The plots at Fig. 15 also demonstrate the basic principle of large number theory. With increasing sample size the associated likelihoods asymptotically reaches zero probability. Also, if an infinite set is theoretically assumed, the critical time history pattern can be identified using deterministic study of the problem. This is certainly nothing new; however, the shape of such pattern (similar to that of Fig. 5) would be in direct contradiction to the definition of stochastic process as observed in reality. Estimating likelihood of such or similarly shaped smooth patterns can be considered controversial, especially for practical purposes, also in comparison to the first passage probability concept.

## 7. Conclusions

A novel **S**mall **T**raining **S**et strategy has been proposed enabling the identification of critical samples of stochastic oscillatory processes from a finite set with respect to the response of a given mechanical model. Such processes are understood here as environmental loads acting on a structural system. From a design point of view, it is essential to identify what particular realization of such a process has critical impact on the structural response. A given dynamical system has a different and unique response to different realizations of the input stochastic loads. Consequently, for Monte-Carlo-based structural reliability considerations, a very large number of realizations of the stochastic load must be considered and analyzed, making the task computationally unfeasible for realistic failure probabilities, since no sampling technique capable of reducing such a task is currently available.

Motivated by the last statement, an importance sampling strategy can be formulated such that it reduces the size of the computational task without sacrificing any of the desirable properties of a fully probabilistic approach. As demonstrated in the numerical examples, identification is feasible with varying performance according to the type of process-model combination considered. As can be observed in Fig. 11, there is no relationship between the complexity of the process-model combination and the performance index.

Successfully tested for both stationary and non-stationary processes, as well as for linear and non-linear mechanical models, an important consequence is that the proposed STS strategy moves the advantages of a fully probabilistic approach within the context of dynamical systems one step closer to engineering practitioners, motivated by the ever-growing demand for performance-based design. Beyond the engineering community, the proposed STS strategy may prove to be a useful technique in the context of environmental sciences, such as water resources, addressing analogous problems such as identifying critical precipitation events.

Further research will focus on possible extensions and improvements regarding the accuracy of the first passage probabilities as well as the treatment of more complex engineering models in the field of structural dynamics and hydrology.

## Acknowledgments

The first author would like to acknowledge the financial support from the Austrian Science Funds (FWF) as part of the Vienna Doctoral Programme on Water Resource Systems (DK-plus W1219-N22) and

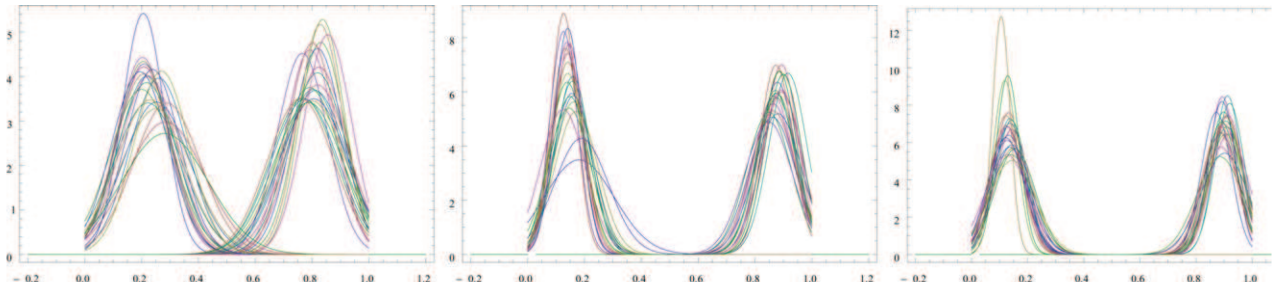

Fig. 12. Separation growth of PDFs (same meaning as in Eq. (10)) for (L1M2 combination) with increasing sample size $n$ (from left to right: $n = 100$, 500 and 1000).

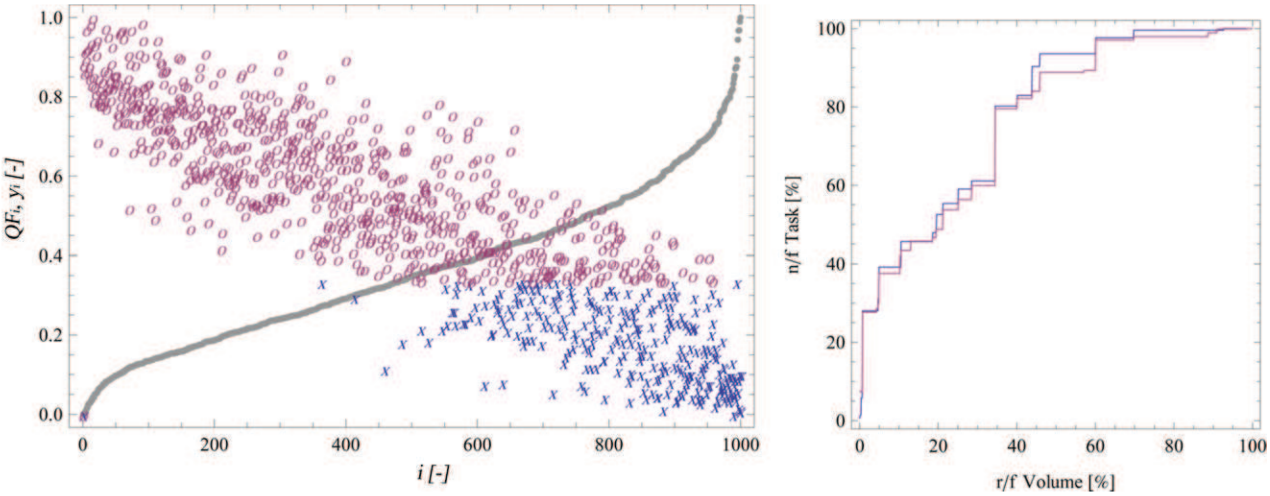


Fig. 13. Left: inverse property of ranked critical response $y_i$ and the quantified important features $\boldsymbol{QF}_i$ (both rescaled to (0, 1) vs. sample size 1000, $S_{ti}$). Here for illustration $q = 10$ and corresponding critical input markers are denoted by "$x$", others by "$o$". Right: percentage of $n$ecessary/$f$ull computational effort as a function of $y_i$ ranked maxima ($r$equired/$f$ull volume) for 2 color channels (R**GB**).

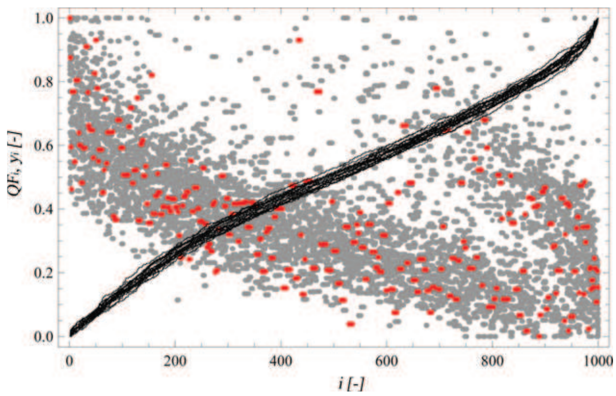


Fig. 14. Rescaled distribution of $y_i$ points (gray cloud) according to ranked $QF_i$ (black lines) from 21 individual realizations (particular realizations denoted by red points); note the emergent 2nd branch STS artifact on the right hand side of the plot). (For interpretation of the references to color in this figure legend, the reader is referred to the web version of this article.)

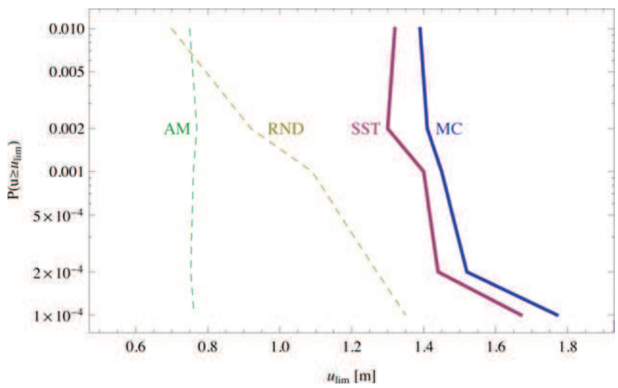


Fig. 15. Determination of probability of exceeding a critical displacement threshold $u_{lim}$ at different sample size scales: comparison of reference brute force Monte Carlo method (100% computational cost) and STS based importance sampling at 1,5% computational costs. Further, random sampling at the same cost as STS is denoted as RND and arithmetic mean of the MC displacements, i.e. not maximum values, as AM.

the hospitality of the Department of Civil Engineering and Engineering Mechanics at Columbia University, NY, where part of the research was conducted. The third author wishes to acknowledge the support provided by the National Science Foundation under Grant No. CMMI-0928129 with Dr. Mahendra P. Singh as Program Director.

## References

[1] Novak D, Strauss A, Bergmeister K, Hoffman S, Pukl R. Advanced life-cycle analysis of existing concrete bridges. J Mater Civil Eng 2008;20(1):9–19.

[2] Podrouzek J, Strauss A, Bergmeister K. Robustness based performance assessment of a pre-stressed concrete bridge. Structural Concrete, Wiley-vch 2013:1751–7648, 10.1002/suco. DOI 201300002.

[3] Priestley MB. Non linear and non stationary time series analysis. Academic Press; 1988, 237.

[4] Moustafa A. Damage-based design earthquake loads for single-degree-of-freedom inelastic structures. J Struct Eng, ASCE 2011:456–467. ISSN 0733-9445.

[5] Takewaki I. Probabilistic critical excitation method for earthquake energy input rate. J Eng Mech, ASCE 2006:990–1000. ISSN 0733-9399.

[6] Barbato M, Conte JP. structural reliability applications of nonstationary spectral characteristics. J Eng Mech, ASCE 2011:371–382. ISSN 0733-9399.

[7] Macke M, Bucher Ch. importance sampling for randomly excited dynamical systems. J Sound Vibr 2003;268:269–90.

[8] Ang AH, Tang WH. Probability concepts in engineering planning. 2nd ed. John Wiley; 2007.
[9] Bamer F, Bucher C. Application of the proper orthogonal decomposition for linear and nonlinear structures under transient excitations. Acta Mechanica 2012;223:2549–63.
[10] Priestley MB. Evolutionary spectra and non-stationary processes. J R Stat Soc, Ser B (Methodological) 1965;27(2):204–37.
[11] Wolfram Mathematica Documentation Center. ref/WaveletScalogram; 2011.
[12] Tezcan J. Nonlinear system response to nonstationary input processes using harmonic wavelets.A thesis submitted in partial fulfillment of the requirements for the degree Doctor of Philosophy. Houston, Texas: Rice University; 2005.
[13] Bay H, Ess A, Tuytelaars T, van Gool L. SURF: speeded up robust features. Comput Vis Image Understan (CVIU) 2008;110(3):346–59.
[14] Drenick RF. The critical excitation of nonlinear systems. J Appl Mech 1977:333–6.
[15] DerKiureghian A. The geometry of random vibrations and solutions by FORM and SORM. Probabilist Eng Mech 2000;15(1):81–90.
[16] Bucher C. Computational analysis of randomness in structural mechanics. In: DM Frangopol, editor. Structures and infrastructures book series, vol. 3. London: Taylor & Francis; 2009.
[17] Clough RW, Penzien J. Dynamics of structures. McGraw-Hill; 1975.
[18] Deodatis G, Shinozuka M. Auto-regressive model for non-stationary stochastic processes. J Eng Mech, ASCE 1988;114(11):1995–2012.
[19] Shinozuka M, Deodatis G. Simulation of stochastic processes by spectral representation. Appl Mech Rev 1991;44:191, 10.1115/1.3119501.
[20] Deodatis G. Non-stationary stochastic vector processes: seismic ground motion applications. Probabilist Eng Mech 1996;11(3):149–67.
[21] Ch. Bucher, Optimal probabilistic design of friction-based seismic isolation devices. Safety, Reliability and Risk of Structures, Infrastructures and Engineering Systems – Furuta, Frangopol & Shinozuka (eds), © 2010 Taylor & Francis Group, London, ISBN 978-0-415-47557-0.

*Chapter 3: Research paper published in Journal of Mechanics Engineering and Automation*

**Importance Sampling Strategy for Oscillatory Stochastic Processes**

Jan Podrouzek

http://www.davidpublishing.com/DownLoad/?id=11162

Publication History
Accepted manuscript online: 25 NOV 2012
Manuscript Accepted: 30 SEP 2012
Manuscript Received: 30 AUG 2012

Editor: Yuping He (Canada)

Online ISSN: 2159-5275

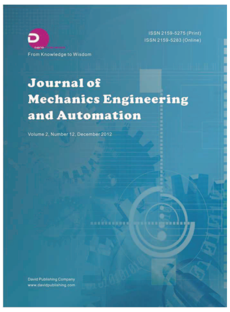

Journal of Mechanics Engineering and Automation 2 (2012) 663-670

# Importance Sampling Strategy for Oscillatory Stochastic Processes

Jan Podrouzek

*Centre for Water Resource Systems (CWRS), Vienna University of Technology, Austria*

Received: August 30, 2012 / Accepted: September 30, 2012 / Published: November 25, 2012.

**Abstract:** This paper contributes to the structural reliability problem by presenting a novel approach that enables for identification of stochastic oscillatory processes as a critical input for given mechanical models. Identification development follows a transparent image processing paradigm completely independent of state-of-the-art structural dynamics, aiming at delivering a simple and wide purpose method. Validation of the proposed importance sampling strategy is based on multi-scale clusters of realizations of digitally generated non-stationary stochastic processes. Good agreement with the reference pure Monte Carlo results indicates a significant potential in reducing the computational task of first passage probabilities estimation, an important feature in the field of e.g., probabilistic seismic design or risk assessment generally.

**Key words:** Stochastic process, critical excitation, reliability analysis, importance sampling, image processing, pattern recognition, identification problem.

## 1. Introduction

The necessity for adopting probabilistic design concepts has become imperative among the structural static problems [1-3]. On the other hand, structural dynamics is still far from practical utilizations of such concepts despite cheap contemporary computational costs. Among the main reasons is the uncertain nature of environmental loading that has to be modeled as a time-varying phenomena, represented in this paper by non-stationary stochastic oscillatory process as an analogy to earthquake event.

It is a well-accepted fact that structures respond in a very uncertain manner to different ground motion events while there is very limited a priori knowledge on the structural behaviour. Same applying for models, an implication is the necessity to perform the structural analysis for each realization of the event separately, which makes the Monte-Carlo (MC) based reliability analysis computationally unfeasible for realistic assumptions, i.e., small probabilities and large sample sizes.

There have been several recent attempts to avoid such reliability problem in its full form. Moustafa [4] proposed a framework for deriving optimal earthquake loads expressed as a Fourier series. More widely, critical excitation methodologists propose to identify critical frequency content of ground motions maximizing the mean earthquake energy input rate to structures (Refer to Ref. [5] for details). From a different perspective, Barbato et al. [6] approximates the first passage problem by formulating exact closed form solutions for the spectral characteristics of random processes. Macke et al. [7] presents an importance sampling technique for randomly excited dynamical systems.

The author of this paper attempt to, unlike the above, maintain the up-to-date most conceptually correct fully probabilistic concept [1] while reducing the number of required analyses by means of the proposed identification framework (designated STS). It is based on a non-traditional assumption that there exists a finite

**Corresponding author:** Jan Podrouzek, doctoral student, research fields: environmental modeling, water resources, stochastic processes, reliability, deterioration, nontraditional numerical techniques. E-mail: podrouzekj@gmail.com.

set of rules capable of classifying synthetic samples of stochastic processes according to their importance as a critical input for given mechanical model. Whether such set of rules could be formulated for arbitrary system remains an open problem for further research.

The paper is organized as follows: In section 2, the development of the proposed method is described; the following section 3 describes the structural and acceleration models; the performance of the method is discussed in section 4; implications for importance sampling strategy follow in section 5 and conclusions are drawn in section 6.

## 2. Development

The identification strategy development follows a transparent image processing paradigm completely independent of state-of-the-art structural dynamics, thus representing a non-traditional option in the field. Reason behind such premise is experimental, aiming at delivering simple and wide-purpose method. The goal can be formulated as follows: to find the critical realization ($S_{T,\ Crit}$) of a stochastic process (S) from a target sample set $S_T$ under defined critical response ($C_r$) criteria.

Proposed STS strategy steps:

(1) Construct a training sample set $S_t$ of size $S_t << S_T$;

(2) Solve the mechanical model (i.e., carry out a structural dynamic analysis): $S_t$ -> $C_r$, usually extremely computationally expensive, therefore the size of $S_t$ should be as small as possible;

(3) Select a proper graphical representation G of $S_t$ (in time domain), which should serve for automatic feature extraction in the next step. There are two general options maintaining the physicality of $S_t$ -> $GS_t$, transformation of $S_t$ into evolutionary spectra [8] or wavelet-vector coefficients based scalogram (Fig. 1) [9], both as 2D graphical arrays. The computational complexity of this task should be minimized, therefore small resolution is desired;

(4) Find a finite set of rules R such that consistently maps $R(GS_t)$ -> $C_r$. Narrow the search domain by ignoring pixels with constant or random-behaviour.

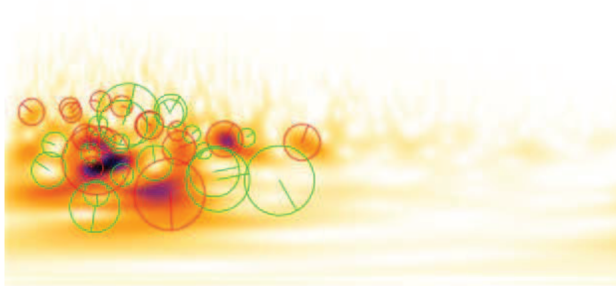

**Fig. 1 Graphical representation (G) of L1 in a form of wavelet scalogram and visualized detected keypoints (R) using their scale (radius of the circle), orientation and contrast sign (color).**

Include pixels into R for which the difference of state values between upper and lower 5th percentile of the ranked $GS_t$ : $C_r$ is maximized;

(5) Obtain $S_{T,\ Crit}$ by applying R -> $S_T$.

In the broader context one should use the STS strategy to limit the number of necessary executions of numerical analysis of the mechanical model. It is assumed that mechanisms behind rules extracted from reasonably small samples are applicable to arbitrarily larger sample. Clearly, whenever using a black-box type of approach, there is a risk of extracting mechanisms that apply only to the training sample if its sample size is too small or in cases of “statistical bad luck”. The determination of minimal size of a training set should be based on a requirement for STS’s predictive confidence.

As stated before, the proposed STS strategy aims at general and automated feature extraction. It should be noted here however that rare instances where experienced when visual comparison of the ranked scalograms G itself enabled for formulation of identification rule R by comparing the number of regions with steep contrast gradient, i.e., image keypoints. For such feature a number of standardized algorithms exists, e.g., implemented Speeded-Up Robust Features (SURF) [10], numerically robust against translation, rotation and scale changes. Such approach can be interpreted as assessment of localized of energy in the time domain and proved to be consistent for configurations of Single Degree Of Freedom (SDOF) oscillators loaded by stationary or amplitude modulated processes. In such instances a low number of detected keypoints indicates a critical process, i.e., G has minimal scatter of excitation energy (See Fig. 2 for example).

The most general non-physical version of STS utilizes several pixels of small-resolution wavelet scalograms image for composition of R and R($GS_t$) -> $C_r$ mapping (step 4) based on a stochastic sensitivity analysis, returning pixels with state values that varies systematically according to the ranked small sample training sets (See Fig. 3).

The sensitive pixels are usually in clusters forming a line (indicating a dominant scale) and/or points (Fig. 3). Regardless of the attractiveness of emerging questions on physical connections of these clusters to the mechanical models (and dominant frequencies), such debates will not be detailed here due to the limited scope of the paper.

## 3. Acceleration and Structural Models

For validation of STS method four distinct combinations of two models (M1 and M2) and loadings (L1 and L2) are considered. The mechanical models represent a single degree of freedom (SDOF) damped linear oscillator (M1) and nonlinear seismically isolated SDOF on a friction pendulum system (M2) subjected to an earthquake loading $F(t) = -ma(t)$. Here $a(t)$ is the ground acceleration described as (L1) an amplitude modulated random process

$$a(t) = e(t) \cdot b(t) \quad (1)$$

where $e(t)$ is the amplitude modulating function given by

$$e(t) = 4[\exp(-0.25t) - \exp(-0.5t)] \quad \text{for } t > 0 \quad (2)$$

and $b(t)$ denotes the stationary zero-mean Gaussian random process with power spectral density:

$$S_{bb}(\omega) = S_0 \frac{4\zeta_g^2\omega_g^2\omega^2 + \omega_g^4}{(\omega_g^2-\omega^2)^2 + 4\zeta_g^2\omega_g^2\omega^2} \quad (3)$$

and as (L2) an amplitude and frequency modulated random process whose objective is to reproduce the general frequency variation characteristics of the

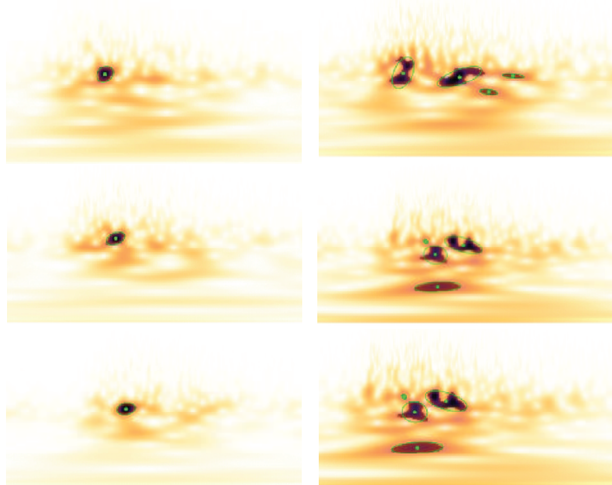

Fig. 2 Number of fitted oriented ellipses (based on SURF) as a performance indicator, left column: 3 ranked maximum and (right column) 3 ranked minimum response.

Fig. 3 Left: Array of pixels (rescaled) according to their behaviour, darker the color, more sensitive the pixel is to the ranked Gs, lighter colors indicates random or invariant behaviour; right: corresponding position of the sensitive pixel at the wavelet scalogram.

acceleration record from the 1964 Niigata earthquake [11] described by the Bogdanhoff-Goldberg-Bernard (1961) envelope function:

$$A(t) = a1\, t \exp(-a2\, t) \qquad \text{for } t > 0 \quad (4)$$

and Clough-Penzien acceleration spectrum with parameters $S_0, \omega_g$ and $\zeta_g = \zeta_f$ as functions of time:

$$S(\omega,t) = S_0(t)\left[\frac{1+4\zeta_g^2(t)\left[\frac{\omega}{\omega_g(t)}\right]^2}{\left\{1-\left[\frac{\omega}{\omega_g(t)}\right]^2\right\}^2+4\zeta_g^2(t)\left[\frac{\omega}{\omega_g(t)}\right]^2}\right]\times \left[\frac{\left[\frac{\omega}{0.1\omega_g(t)}\right]^2}{\left\{1-\left[\frac{\omega}{0.1\omega_g(t)}\right]^2\right\}^2+4\zeta_f^2(t)\left[\frac{\omega}{0.1\omega_g(t)}\right]^2}\right] \quad (5)$$

$$S_0(t) = \frac{\sigma^2}{\pi\,\omega_g(t)\left(2\zeta_g(t)+\frac{1}{2\zeta_g(t)}\right)} \quad (6)$$

$$\omega_g(t) = \begin{cases} 15.56, & 0 \le t < 4.5 \\ 27.12\,(t-4.5)^3 - 40.68(t-4.5)^2 + 15.56, & 4.5 \le t < 5.5 \\ 2.0, & t \ge 5.5 \end{cases} \quad (7)$$

$$\zeta_g(t) = \begin{cases} 0.64, & t < 4.5 \\ 1.25\,(t-4.5)^3 - 1.875(t-4.5)^2 + 0.64, & 4.5 \le t < 5.5 \\ 0.015, & t \ge 5.5 \end{cases} \quad (8)$$

where parameters $a1$ = 0.68, $a2$ = 0.25 and $\sigma$ = 100.

The nonlinear mechanical model M2 represents a building (SDOF) combined with a friction based seismic isolation (friction pendulum system) device that introduces another mechanical degree of freedom as well as an internal variable representing plastic slip $z$. The implementation was adopted from Ref. [12] and will not be detailed in this paper. The structural data for both M1 and M2 are provided in Table 1, random realizations of L1 and L2 and response characteristics are depicted in Fig. 2.

Critical response criterion was formulated either as absolute values of top displacement of mass most distant from the application of seismic load or as given percentile of the mean-square values of the displacements. The former criterion led to better identification performance and therefore was adopted.

## 4. Identification Results

Development and testing of the STS on multiple scales and process-model scenarios showed that it is difficult, perhaps impossible, to formulate a general identification rule of physical interpretability, a fact that corresponds with the structural dynamics paradigm. One of such attempts led to the formulation of R incorporating the image keypoints as a way of quantifying the energy scatter in the loading process. Therefore, soft computing techniques were deployed in search for general black-box type method. The presented state of STS was tested on large number of clusters composed from a total of $4.2 \times 10^4$ realizations of Kt and Ni process in combination with various mechanical models (For sample realization see Fig. 4). The stochastic simulations revealed the existence of R for every tested process-model scenario. Results presented in Fig. 5 were chosen to demonstrate the variability of performance and do not represent the best nor worst analysed process-model instances.

The performance index was defined according to the following integral:

**Table 1 Mechanical models M1 & M2 (left, right) and structural data.**

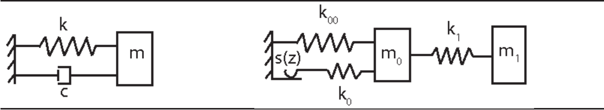


| | | | |
|---|---|---|---|
| | | $m_0$ | 6080 kg |
| m | 400 kg | $m_1$ | 79770 kg |
| k | 80 MN/m | $k_0$ | 42372 KN/m |
| c | 120 | $k_{00}$ | 2629 KN/m |
| | | $k_1$ | 62500 kN/m |

$$P = \int_0^1 PDF_{min}(x).PDF_{max}(x)dx \quad (9)$$

where $PDF_{min/\max}$ states for the probability distribution function fitted to the ranked minimum/maximum set, growing isolation of these functions indicates better performance (See Fig. 6). The integration range corresponds to the admissible value of the G pixels.

## 5. Importance Sampling

Following a successful formulation and validation of R according to the proposed STS, the importance sampling strategy is based on applying R to the full (original) set of realizations of stochastic processes and sorting the functional values of this product. Finally, the first $n$ realizations corresponding to the ranked set are determined as critical input for numerical models. The determination of $n$ depends on the required Importance Sampling confidence, e.g., in the presented case study (KtM2 model-process scenario) $n$ = 10, i.e., 1% of the full set (1000) (See Figs. 7-8).

The importance sampling test scenario, as described above, proved to be a consistent measure for reducing the 1000 sample set to a smaller set while maintaining the same critical response characteristics. The STS utilized 100 sample training set (10%) and the consequent importance sampling required additional 10 analyses (1%), therefore reducing the computational task by 89%. The additional 1% ensured that the important sample (most critical response) was captured by over 91% (within 21 test runs). Note the effect of emergent 2nd branch STS artefact from Cr distribution plot according to ranked R product. The inverse of the same plot (Fig. 7) does not exhibit such effect, representing the amount of

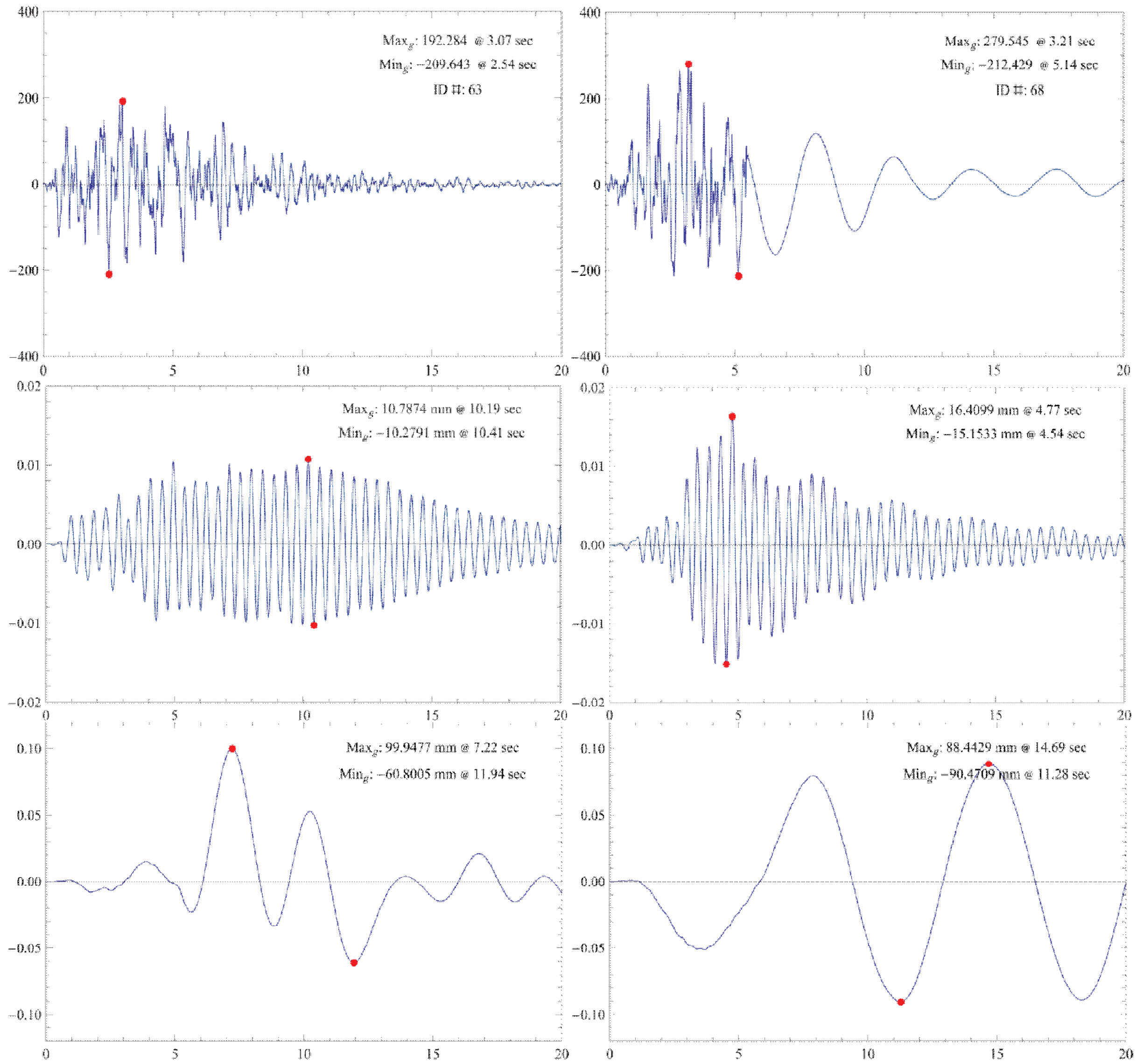


**Fig. 4** Example of realizations: left column top down: L1 process, M1 and M2 response to L1; right column top down: L2 process, SDOF response to L2, FPS response to L2 (note the abrupt change of frequency content at 5.5 sec); time at horizontal axes, acceleration/displacement on vertical axes.

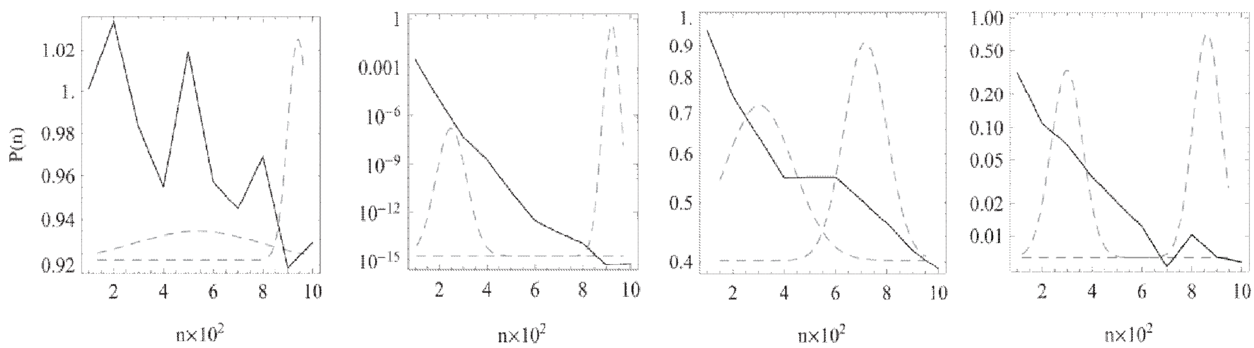


**Fig. 5** Performance index P as a function of sample size n, left to right: KtM1, KtM2, NiM1, NiM2; dashed line represents the normal distribution PDFs fitted to 21 joined min and max sets for sample size $n = 2.1 \times 10^4$; Note the PDFs spacing effect on performance index.

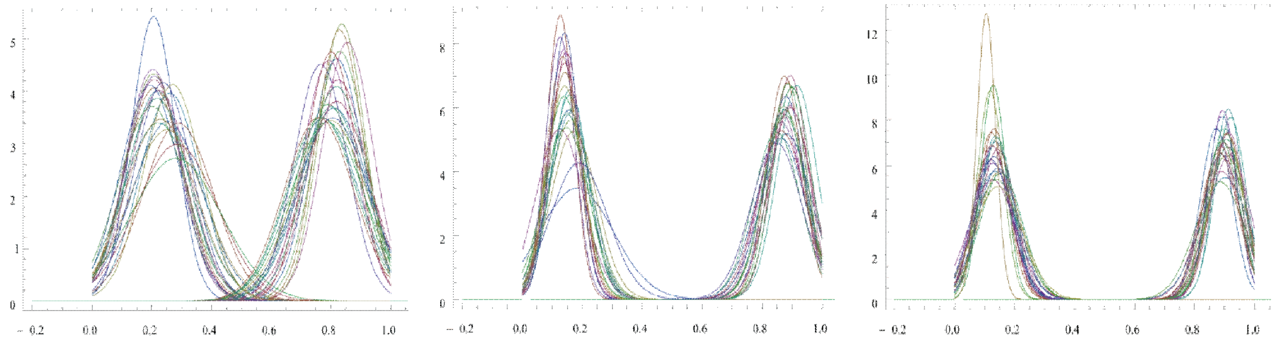

**Fig. 6** **Ranked sets PDF {min, max}; Isolation growth with increasing sample size *n* = {100, 500, 1000}; KtM2 realizations.**

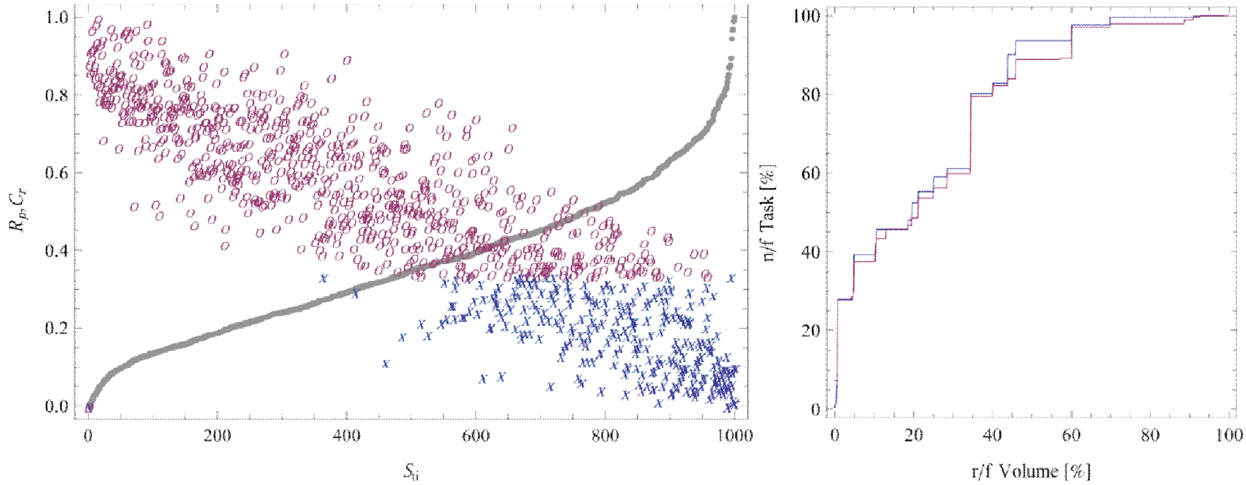


**Fig. 7** **Left: Inverse property of ranked critical response ($C_r$ points) and the R product (both Rescaled to (0, 1) vs. sample size 1000, $S_{ti}$); here for illustration *n* = 10 and corresponding critical input markers "x", others "o". Right: Percentage of necessary/full computational task as a function of $C_r$ ranked maxima (required/full volume) for 2 colour channels (RGB).**

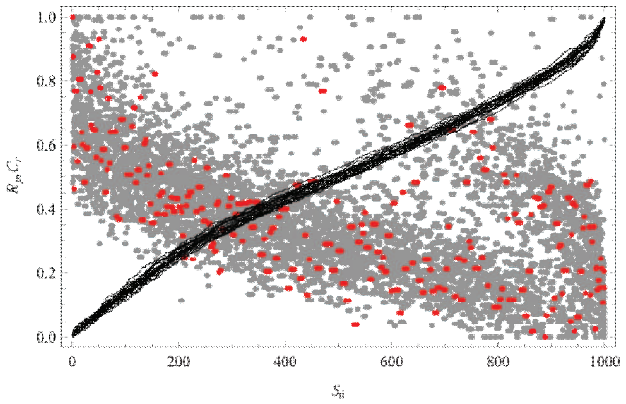


**Fig. 8** **Rescaled distribution of $C_r$ points (gray cloud) according to ranked R product (black line) from individual realizations $S_{ti}$; 21 repeated runs; particular realization in red points; note the emergent $2^{nd}$ branch STS artefact.**

unaccounted information by STS. This is partly due to (1) incorporating only one sensitive point and (2) ambiguous $C_r$ -> $R_p$ identifier based RGB (Red, Green and Blue) channels. The performance of STS could be enhanced by including multiple sensitive points with cross-correlations (1) and by modifying the R products by labels (e.g., random binary sequencing) or by enhancing the colour depth to ensure uniqueness (2).

The effect of unaccounted information does not only exhibit itself via the $2^{nd}$ branch, but clearly also by the inability to always capture the single $C_r$ maximum, as one might observe on the comparison plot in Fig. 9. Here the goal was to determine the probability of exceeding a critical displacement threshold $u_{lim}$ at different sample size scales and compare it against reference pure Monte Carlo values. In terms of accuracy the maximum reached deviation between the MC reference and SST value was 15%, however, in terms of computational efficiency the STS based importance sampling utilized only 4.6% of the MC computational cost, i.e., 0.6% for feature extraction and the remaining 4% for running the *n* realizations

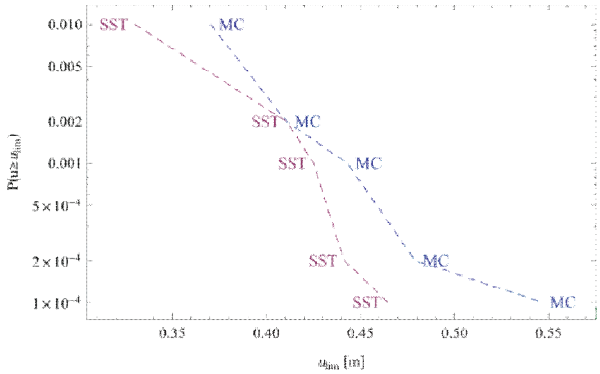


**Fig. 9 Determination of probability of exceeding a critical displacement threshold $u_{lim}$ at different sample size scales: Comparison of pure Monte Carlo method (100% computational costs)and STS based importance sampling at 4.6% of computational cost.**

corresponding to the $P_r$ ranked sets. This result indicates that there is significant potential in the application of the STS approach to the estimation of first passage probabilities. Nevertheless, the accuracy in its present form is not comparable to established simulation techniques. Due to its substantial computational advantage, however, the present approach will be suitable especially for reliability-based design optimization in which the reliability analysis has to be repeated frequently.

## 6. Conclusions and Discussion

A novel Small Training Set (STS) strategy proposed by the author enables for identification of critical stochastic oscillatory processes with respect to given mechanical model. Such process is understood here as an environmental load acting on a structural system. From a design point of view, it is essential to understand what particular realization of such process has the critical impact on the structure. Traditionally, it is understood that each individual dynamical system has a very unique response to various stochastic loads. Therefore, for Monte-Carlo-based structural reliability considerations, all realizations of the stochastic load must be executed individually, making the task computationally unfeasible for realistic failure probabilities, since no sampling technique capable of reducing such task is available up to current date.

Motivated by the latter statement, an importance sampling strategy is formulated such that it reduces the size of the computational task without sacrificing any of the properties of fully probabilistic approach. As demonstrated on the numerical examples, the identification is feasible with varying performance according to the type of process-model scenario. As one may observe in Fig. 5, there is no relationship between the complexity of the process or model and the performance index.

Positively tested for both stationary and non-stationary processes, linear and non-linear mechanical models, an important implication is that the proposed STS strategy moves the fully probabilistic approach within the context of dynamical systems one step closer to the engineering practitioners, motivated by the ever-growing demand for performance-based design. Besides from the engineering community, STS may be a useful technique in the context of environmental sciences, such as water resources, solving analogous problems, e.g., realistic critical precipitation scenarios.

Further research will focus on possible extensions and improvements regarding the accuracy of the first passage probabilities as well as the treatment of more complex engineering models including structural dynamics and hydrology.

## Acknowledgment

The author would like acknowledge the financial support from the Austrian Science Funds (FWF) as part of the Vienna Doctoral Programme on Water Resource Systems (DK-plus W1219-N22) and the hospitality of the Department of Civil Engineering and Engineering Mechanics at Columbia University, NY, where part of the research was conducted, especially Prof. Deodatis for inspiring discussions.

## References

[1] A.H.-S. Ang, W.H. Tang, Probability Concepts in Engineering Planning and Design, John Wiley & Sons, New York, 1990.

[2] A. Haldar, S. Mahadevan, Reliability Assessment Using Finite Element Analysis, John Wiley & Sons, New York, 2000.

[3] R.E. Melchers, Structural Reliability Analysis and Prediction, 2nd ed., John Wiley & Sons, Chichester, 2001.

[4] A. Moustafa, Damage-based design earthquake loads for single-degree-of-freedom inelastic structures, Journal of Structural Engineering 137 (2011) 456-467.

[5] I. Takewaki, Probabilistic critical excitation method for earthquake energy input rate, Journal of Engineering Mechanics 132 (2006) 990-1000.

[6] M. Barbato, J.P. Conte, Structural reliability applications of nonstationary spectral characteristics, Journal of Engineering Mechanics 137 (2011) 371-382.

[7] M. Macke, Ch. Bucher, Importance sampling for randomly excited dynamical systems, Journal of Sound and Vibrations 268 (2003) 269-290.

[8] M.B. Priestley, Evolutionary spectra and non-stationary processes, Journal of the Royal Statistical Society: Series B (Methodological) 27 (2) (1965) 204-237.

[9] Mathematica, Version 7.0, Wolfram Research, Inc., Champaign, IL, 2008.

[10] H. Bay, A. Ess, T. Tuytelaars, L. Van Gool, SURF: speeded up robust features, Computer Vision and Image Understanding (CVIU) 110 (3) (2008) 346-359.

[11] M. Shinozuka, G. Deodatis, Simulation of stochastic processes by spectral representation, Appl. Mech. Rev. 44 4 (1991) 191-204.

[12] Ch. Bucher, Optimal probabilistic design of friction-based seismic isolation devices, in: H. Furuta, D.M. Frangopol, M. Shinozuka (Eds.), Safety, Reliability and Risk of Structures, Infrastructures and Engineering Systems, Taylor & Francis Group, London, 2010.

*Chapter 4: Technical paper published in Structural Concrete Journal*

**Robustness based performance assessment of a pre-stressed concrete bridge**

Jan Podrouzek, Alfred Strauss, Konrad Bergmeister

DOI: 10.1002/suco.201300002

Publication History
Accepted manuscript online: 6 NOV 2013
Manuscript Accepted: 4 OCT 2013
Manuscript Revised: 3 SEP 2013
Manuscript Received: 14 JAN 2013

Editor-in-Chief: Luc Taerwe (Belgium); Deputy Editor: Steinar Helland (Norway)
Impact Factor: 0.289
ISI Journal Citation Reports © Ranking: 2012: 46/57 (Construction & Building Technology); 105/122 (Engineering Civil)

Online ISSN: 1751-7648

Jan Podroužek
Alfred Strauss*
Konrad Bergmeister

DOI: 10.1002/suco.201300002

# Robustness-based performance assessment of a prestressed concrete bridge

*Life-cycle civil engineering addresses, among other things, the growing number of deteriorating bridges and the associated economic challenges. As a consequence, government bodies, infrastructure and bridge owners as well as industry request objective and rational performance indicators for classification and intervention planning in structural engineering. This paper focuses on a methodology for analysing the damage-based robustness margins of bridge systems under traffic loading. In particular, a series of emergent deterioration-based damage scenarios are compared with the actual or virgin state in terms of loadbearing capacity and serviceability. Non-linear finite element analysis based on a detailed 3D model has a high potential for capturing the available bridge capacity for different degradation phenomena and levels, serving as an input for further reliability-based performance indicators. Notwithstanding, costs associated with fully probabilistic assessment measures are still prohibitive despite technological advances and new methods of reducing the sample size in Monte Carlo computations. In addition, considering the large uncertainties and imprecision involved, it is imperative that probabilistic schemes are preferred over deterministic assessments.*

*The objective of this article is to present strategies for robustness-based performance assessment using non-linear modelling and to discuss relevant reliability-based quantities and performance indicators in relation to structural damage using the example of specific degradation events in an existing prestressed box girder bridge. Furthermore, some strategies are developed on the basis of the new approach for general complex engineering structures.*

**Keywords:** robustness, existing structure, reliability, performance indicators, safety, stochastic methods

## 1 Introduction

Our understanding is still very limited in many fields of life-cycle civil engineering. For instance, concrete deterioration mechanisms such as creep and corrosion have a significant impact on the durability and serviceability of infrastructure systems, but our understanding of the impact of combined actions needs to be improved. Therefore, strategic approaches are needed to establish simple performance assessment procedures with some realistic background analysis. As shown in Fig. 1, it is hardly possible to quantify the likelihood of such combined actions or to define the effect of single risks on the durability. Fig. 1 attempts to illustrate the complex interactions between external action processes and processes within the structure, and the resulting modelling requirements to the extent to which it is generally possible to implement them. As a result of the complexity of such modelling, considerable simplifications are frequently made [1]. The non-linear robustness modelling approach chosen in this contribution virtually makes it possible to isolate the analysis from the causes of the degradation processes. The analysis is based only on existing damage profiles; it assumes a set of deteriorated elements (regions), e.g. the loss of prestressing tendons as definite facts due to corrosion and chloride ingress processes, for example. The set of deteriorated elements has been derived from non-destructive and destructive testing results (e.g. data from [23], [13]) and input gained from consultations with experts. In addition, damage catalogues such as those developed for DIN 1076 have been used to explore the likelihood of deterioration processes associated with the selected set of deteriorated elements. The concept presented addresses the performance-based approach as established in the *fib* Model Code for Concrete Structures 2010, particularly the issues of chapter 9, i.e. conservation strategies, condition assessment and intervention planning [15].

The design and modelling of new or degraded bridges and structures, for example, are traditionally performed on a member-by-member basis [2], [10]. Usually, no consideration is given to the system capacity, which can prove compensatory where some structural elements fail due to degradation processes [3], [7], [8]. In general, the failure of an individual member does not lead to the failure of a complete statically indeterminate structure or bridge system [9], [10], [11], [34], [35].

As a result of the constant increase in the number of deteriorating structures and bridge systems, taking advantage of the system reserves mentioned above as well as the structural robustness is rapidly attracting more interest [14]. Since both system reserves and structural robustness are related to the overall system behaviour, the traditional member-oriented approach fails to provide objective safety margins and global assessment procedures. The system

* Corresponding author: alfred.strauss@boku.ac.at

Submitted for review: 14 January 2013
Revised: 3 September 2013
Accepted for publication: 4 October 2013

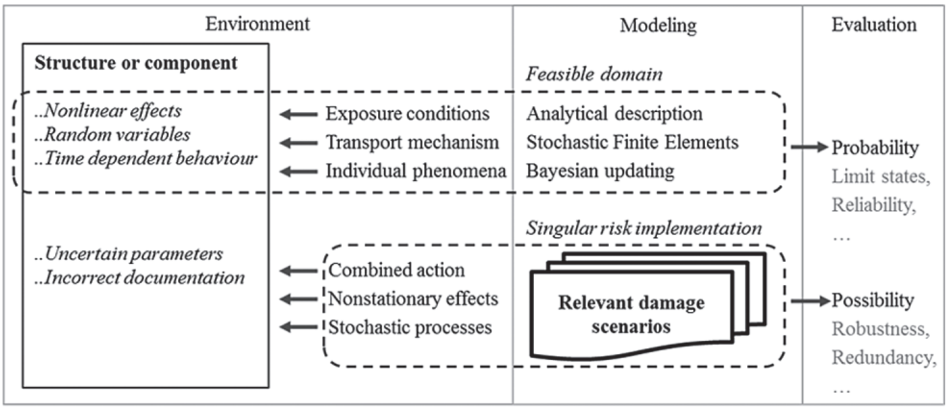


**Fig. 1.** Modelling requirements: interaction between external action processes and processes within a structure, as described in section 2

reserves and structural robustness are of increasing relevance together with non-linear fracture mechanics-based finite element modelling [17], [19], [20], [21], [12] .

In this contribution, non-linear numerical model techniques combined with robustness and redundancy concepts will be discussed in order to capture existing overall system behaviour; in particular, the studies are performed on a selected prestressed bridge structure in South Tirol, Austria. Robustness issues are closely linked with degradation processes, maintenance strategies and hence with the remaining lifetime $t_R$ of structures. Therefore, an additional objective of these studies has been the evaluation of robustness- and redundancy-associated concepts for the determination of $t_R$ with respect to defined degradation phenomena [3]. The degradation processes, considered for the case study mentioned above, have been derived on the basis of bridge inspection measures and in respect of the EN 1991 load model LM1. In particular, the LM1 loading levels associated with (a) first member failure, (b) ultimate capacity of damaged system and (c) loss of functionality and ultimate capacity of the intact system are investigated. Linear as well as non-linear modelling techniques have been used in order to characterize the system behaviour and associated failure mechanisms comprehensively [22], [29], [30], [31]. In particular, fundamental differences in the failure mechanisms were observed with respect to the modelling methods. The factor $\gamma_{LM1}$ used in these studies refers solely to the variable values of load model LM1 and represents the loading percentage.

The system redundancy and robustness mentioned above are defined differently by different authors. Accordingly, the **redundancy** (Latin: "redundare": to overflow, to abound) of a system defines the multiple presence of functionally identical or similar technical resources (load reserves) and the ability of the system to continue to carry load after the capacity of individual members is exceeded or even after the removal of individual members from the system. According to [10], [11] , redundancy is defined as the capability of a system to redistribute and increase loading processes after the failure of one main member. As a provision of capacity, a redundant structure has additional structural capacity and reserve strength, allowing it to carry a higher load than anticipated when considering the capacity of individual members. The measures of redundancy are:

$$R_u = LF_u \,/\, LF_1 \tag{1}$$

$$R_f = LF_f \,/\, LF_1 \tag{2}$$

$$R_d = LF_d \,/\, LF_1 \tag{3}$$

where:
$LF_1$ load that causes failure of the first member
$LF_u$ load that causes collapse of the system
$LF_f$ load that causes the functionality limit state of the initially intact structure to be exceeded
$LF_d$ load factor that causes the collapse of a damaged structure that has lost one main member

An alternative definition associated with the redundancy of a system was also given in terms of the reliability index using a "redundancy factor" $\beta_R$:

$$\beta_R = \frac{\beta_{int.}}{\beta_{int.} - \beta_{damaged}} \tag{4}$$

where:
$\beta_{int.}$ reliability index of intact structural system
$\beta_{damaged}$ reliability index of damaged structural system

Note that his type of analysis can only be implemented in cases where appropriate data regarding the potential hazards (actions, degradation) are available and where the system reliability indexes associated with these events can be determined reliably. Probabilistic finite element software packages such as the "Structural Analysis and Reliability Assessment (SARA)" developed by Cervenka Consulting [17], [21], [12] or the software package COSSAN X (http://cossan.co.uk/) are tools well suited to determining an existing system's reliability.

The second term commonly used in connection with system reliability is that of **robustness** (Latin: "robustus", adjective of "robur": oak, very hard wood), which denotes the ability of a system to withstand changes without having to adapt its originally stable structure. Examples are the robustness of a system against overloading or its robustness against a decrease in load-carrying capacity of individual system elements. According to [10], [11], robustness can be considered as the capability to perform without failure under unexpected conditions. *Frangopol*, *Biondini* and *Ghosn* ([10], [11]) have defined robustness on the basis of the following robustness index:

$$RI = \frac{P_{f\,damaged} - P_{f\,intact}}{P_{f\,intact}} \tag{5}$$

where:
$P_{f\,damaged}$ probability of failure of a damaged structure
$P_{f\,intact}$ probability of failure of the intact structure

Obviously, $RI = 0$ for a robust structure and may approach infinity for a non-robust structure. In addition, implementable redundancy and robustness measures were advanced by the offshore industry in the ISO 19902 standards. One of those measures is the Reserve Strength Ratio (RSR), which is defined as

$$RSR = \frac{Q_{ultimate}}{Q_{design}} \tag{6}$$

where:
$Q_{ultimate}$ load capacity of the structure
$Q_{design}$ unfactored design load

Another measure is the Damaged Strength Ratio (DSR), defined as

$$DSR = \frac{Q_{damaged}}{Q_{design}} \tag{7}$$

where:
$Q_{damaged}$ load capacity of a structure damaged due to corrosion or fatigue failure

More details with respect to robustness and redundancy formulations are provided in [10], [11]. In the following, the above observations regarding robustness and redundancy will be applied to a hollow box girder bridge system, followed by the definition of the corresponding performance indicators.

## 2 Definition of bridge and possible damage scenarios

The Colle Isarco Bridge belongs to the complex engineering structures on highway A22, part of the Brenner Highway in northern Italy. This 40-year-old box girder bridge is characterized by its high number of prestressing tendons and its high prestressing degree in all three directions. Owing to the inherent complexity of the system and the high frequency of heavy axle loads [4], there is great interest in the system-specific reliability assessment and performance prediction as provided by the robustness and redundancy approaches discussed above. Fig. 2 shows the configuration of the spans and the topology of the Colle Isarco Bridge, a concrete prestressed box girder structure erected in 1969. The bridge has a total length of 1028.80 m and consists of 13 spans. The deck of the post-tensioned box girder bridge is represented by two parallel box girder superstructures with a total width of 22.10 m, which are supported by the same piers. The bridge was designed as an externally statically determinate structure. The box girders are cast-in-place balanced cantilever beams with varying girder depth. The depth of the box girders varies from 10.80 m over the middle support to 2.85 m at mid-span.

A comprehensive non-linear 3D finite element model was developed within the ATENA software environment for the robustness and redundancy analyses of the Colle Isarco Viaduct (see Fig. 3b) [6]. In particular, the ATENA software tool was chosen since it comprises highly developed material laws for the non-linear investigation of concrete and reinforced concrete. The virtual FE model of the Colle Isarco Bridge includes 496 individual prestressing tendons, i.e. longitudinal parabolic bottom slab tendons, vertical tendons and top slab tendons, all arranged according to the bridge documentation drawings as shown in Fig. 3a. The mild steel reinforcement of the box girder was modelled with a smeared reinforcement approach by assigning the reinforcement ratios in accordance with the original drawings (see Fig. 3a); more details associated with smeared reinforcement approaches are provided in [19]. In total, the finite element model consists of about $9 \times 10^3$ volume elements, as illustrated in Fig. 3b.

The primary objective of the first reliability assessment phase of the Colle Isarco Bridge was to reproduce the original (virgin) real system behaviour as well as the design system behaviour loaded by the self-weight and the LM1 load model of EN 1991. To this end, use was made of the limits specified in the standards that were valid at the

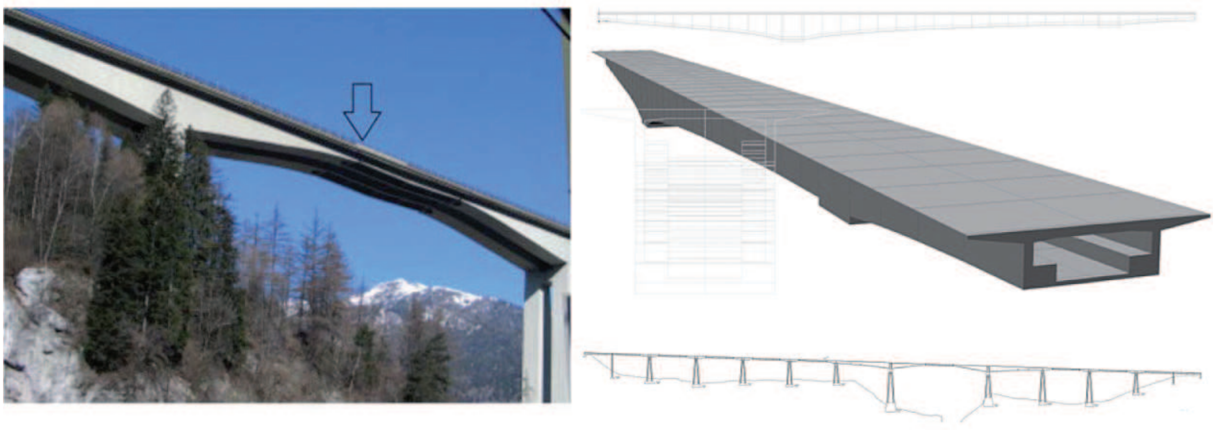

**Fig. 2.** Side view of main girders (l = 163 m) of Colle Isarco Bridge and general overview of Colle Isarco Bridge system. The arrow indicates a significant observation point for deflections, which was frequently used for evaluation measures (longitudinal x coordinate 58.45 m).

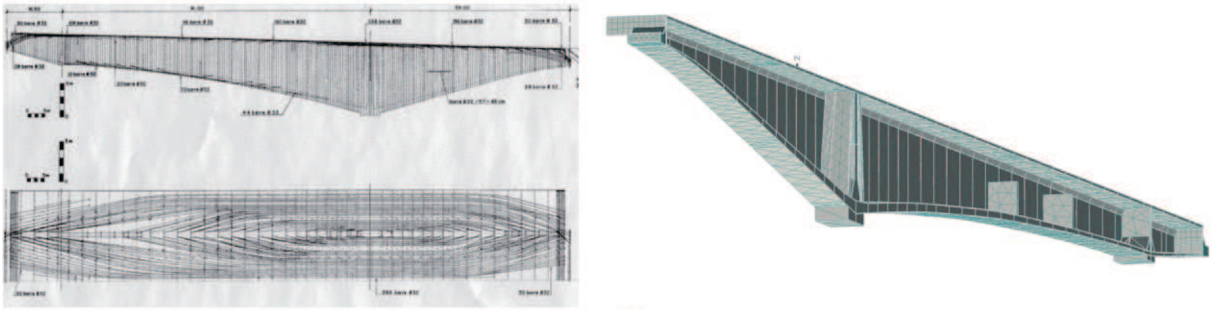


**Fig. 3.** Drawings and FE model of main girder of Colle Isarco Viaduct: (a) geometry of prestressing tendons according to original 1970s documentation and (b) 3D symmetrical FE model

time and the bridge construction records (e.g. pretensioning logs). In order to reduce the simulation errors (= modelling errors and solution error) in the area of idealization and discretization, which can arise during the development of the non-linear FE model, various variations were implemented (see [33]). These included variations in the boundary conditions (level 1 validation), variations in mesh size (level 2 validation) and element type (level 3 validation) as well as variations in the solution process (level 4, verification of solution error). The model updating of the physical FE model associated with this process was performed on the basis of the monitoring data of and with reference to the proof loading that was carried out in the course of the inspection and approval of the viaduct. On the basis of the updated original model, relevant damage scenarios were defined, taking into consideration the inspection data and the outcome of an assessment of the risk that degradation processes pose to the structure. These damage scenarios reflected, among other things, the current and future conditions caused by environmental loading and material deterioration. Significant associated processes are chloride ingress, reduction in concrete cover, reinforcement corrosion, loss of prestressing cables as well as creep and shrinkage processes and their effect on the prestressing system [27]. The inspection data revealed

**Table 1.** Random properties of concrete

| Property [unit] | Mean | PDF | COV |
|---|---|---|---|
| $E$ [GPa] | 30 | lognormal | 0.15 |
| $f_c$ [MPa] | –38.37 | lognornal | 0.10 |
| $f_t$ [MPa] | 2.066 | *Weibull* | 0.18 |
| $G_f$ [MN/m] | 7e-5 | *Weibull* | 0.20 |

**Table 2.** Random properties of steel

| Property [unit] | Mean | PDF | COV |
|---|---|---|---|
| prestressing $E_s$ [GPa] | 210 | lognormal | 0.08 |
| smeared $E_s$ [GPa] | 210 | lognormal | 0.13 |

**Table 3.** Correlation matrix for concrete

| | $E_c$ | $f_c$ | $f_t$ | $G_f$ |
|---|---|---|---|---|
| $E_c$ | 1 | 0.9 | 0.7 | 0.5 |
| $f_c$ | 0.9 | 1 | 0.8 | 0.6 |
| $f_t$ | 0.7 | 0.8 | 1 | 0.9 |
| $G_f$ | 0.5 | 0.6 | 0.9 | 1 |

that the mechanism of chloride propagation in some areas underneath the pavement in the top slab is a result of the application of de-icing salt (diffusive feed). This process had a direct impact on tendons in the top slab.

In order to capture the uncertainties and the scattering values in both the action and the resistance models and to exploit the resulting information in the actual assessment process, the damage scenarios were in many cases examined using non-linear stochastic FE approaches combined with probabilistic characteristics. For the Colle Isarco Bridge, an extensive survey of inspection examination records and relevant literature [13], [23]. [28] indicates the stochastic properties as shown in Table 1. The correlations between the scattering input variables, determined on the basis of relevant literature [26], [31], [16], [25], are listed in Table 3.

The statistical system responses to the probabilistic non-linear FE analyses as shown in Table 4 were of interest for the Colle Isarco Viaduct studies. In particular, the damage scenario depicted conceptually in Fig. 5 is based on the findings of historic inspection activities.

In an initial approach, the complexity of the damage processes was modelled in a simplified manner; simultaneous occurrence and interaction were not considered. Such information is very difficult to generate from purely theoretical considerations or even using simulation and sampling methods. In general, such information can be attained only by judicious implementation of monitoring systems over a longer period of time and on the basis of preliminary surveys [36], [37]. In addition, within a given time frame, it enables the utilization of information available from monitoring, visual inspection and correlation between surface properties and internal mechanical properties.

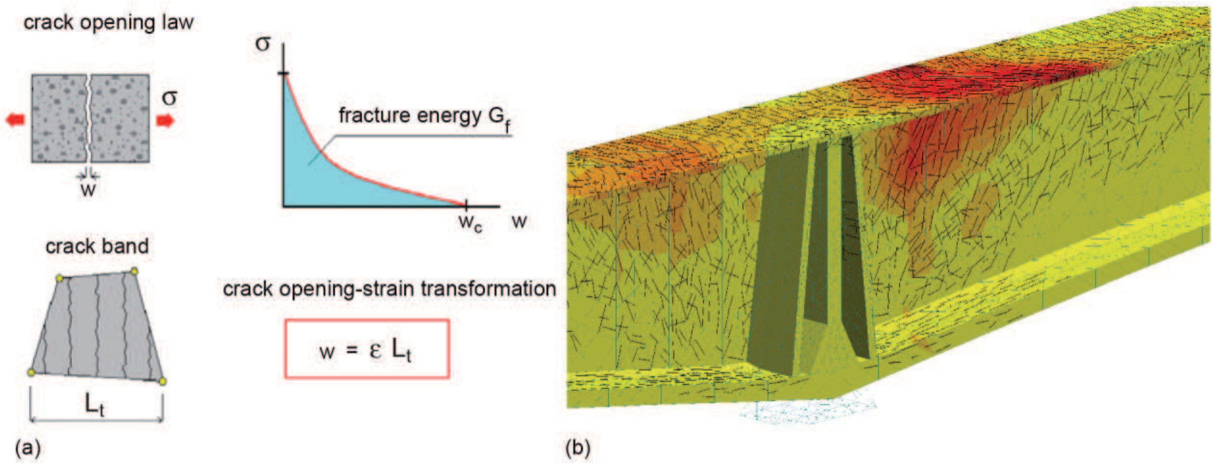


**Fig. 4.** Advanced concrete material models for non-linear finite element analysis: (a) crack band model for smeared crack approach under tension and compression, (b) computed fracture process zone using crack band approach next to support of prestressed Colle Isarco Bridge (red contours represent maximum fracturing strain in longitudinal direction)

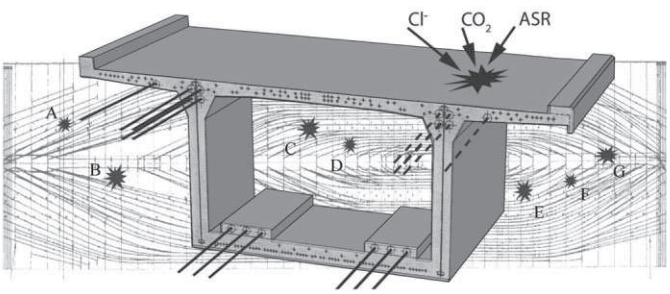


**Fig. 5.** Damage scenario concept: combined chemical action on a bridge superstructure resulting in the loss of particular prestressing tendons (dashed lines) at specific locations (letters A to G) determined on the basis of inspection records; typical cantilever segment with the pretensioned tendon profiles and representation of worst chloride ingress location resulting in the loss of several pretensioned cables (dashed lines)

**Table 4.** Relevant structural responses

| |
|---|
| serviceability limit state |
| deflection |
| ultimate limit state |
| load capacity |
| crack width |
| concrete stress, top slab |
| concrete stress, bottom slab |
| durability limit state |
| crack opening in upper slab surface |
| crack width in exposed areas |
| loss of prestress due to creep |

## 3 Performance assessment

The Colle Isarco superstructure was designed as a statically determinate system. Typical redundant and robust structures are hyperstatic structures and the aim is usually to determine the remaining capacity after the first member failure due to, for example, overloading or continuous or sudden functional failure as a result of degradation processes. For the Colle Isarco Bridge, a structure that is statically determinate externally and, as a result of the pretensioning, statically indeterminate internally to a very high degree, the characteristics related to robustness and redundancy are closely linked with the failure of any of the 494 individual pretensioning cables. The cause of these failures is attributed to chloride ingress as a result of inadequate sealing underneath the road surface. Determination of the expected failure rate of the tendons over time allows indirect conclusions to be drawn regarding the chloride ingress process, as studied by *Teplý* and *Vořechovská* [32], for instance. In addition, statements and information about the future development of traffic are essential for the reliability assessment and, consequently, for estimating the remaining lifetime $t_R$, which has to be considered in combination with increasing traffic flows.

In this context, defining the performance indicators that make it possible to predict the failure and/or a decrease in the load-carrying capacity of structural elements, e.g. the pretensioning elements, at an early stage are of enormous interest. The definition of such performance indicators may be (a) limited to structures of the same type, (b) refer to structural networks or (c) refer to the universally valid mechanical principles. The performance indicators outlined above in relation to the robustness and redundancy of a system can be adopted for standardized frames of reference that provide an objective basis for assessment and decision-making with regard to bridge networks to be used by the structure's owners. In this context, the work of *Ghosn* et al. [10] is relevant. They pursue approaches along these lines and also provide succinct lists of code-specified criteria for evaluating the performance of bridge systems exposed to various types of hazard. In this regard, in the following the probabilistic performance indicator concept will be analysed in detail with regard to its applicability and feasibility in the example of the Colle Isarco Bridge. For the failure scenarios, $ds1$ to $ds3$ are analysed. The first scenario $ds1$ follows degradation evolution-induced (e.g. chloride ingress, see Podroužek et al. [18]) loss of randomly selected prestressing tendons from the upper slab by means of independent sampling. In particular, each probabilistic analysis of the

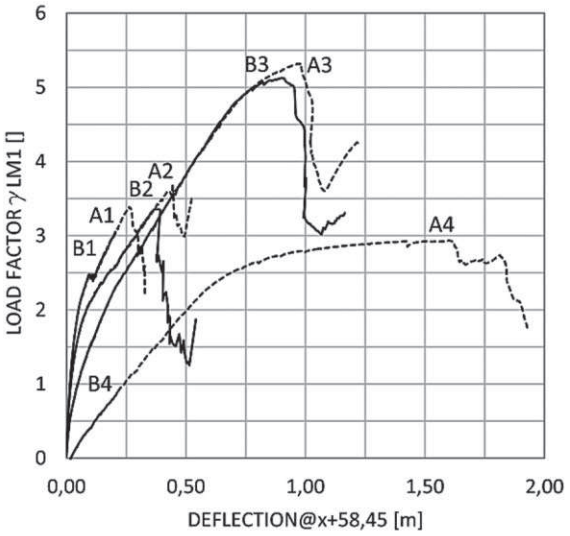


**Fig. 6.** Load-displacement diagram for damage scenario $ds1$, for $A1$ = 0 %, $A2$ = 15 %, $A3$ = 30 %, $A4$ = 45 % loss of prestressing tendons, where $A$ indicates a concrete material permissible strain parameter $e_{ca}$ = 0.2 and $B$ indicates $e_{ca}$ = 0.35

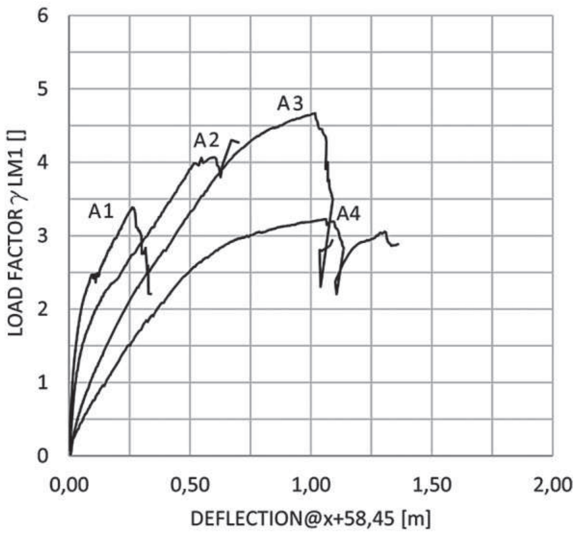


**Fig. 8.** Load-displacement diagram for damage scenario $ds2$ (statistical dependence between the random variables) for $A1$ = 0 %, $A2$ = 15 %, $A3$ = 30 %, $A4$ = 45 % loss of prestressing tendons, where $A$ indicates a concrete material permissible strain parameter $e_{ca}$ = 0.2

damage scenarios investigated was limited to four degrees of failure: case $A1$ = 0 % tendon failure rate, case $A2$ = 15 % failure rate, case $A3$ = 30 % and case $A4$ = 45 % (see Fig. 6). In addition, based on consultations with experts, a distinction was made between variant $A$ = concrete material permissible strain parameter, i.e. $e_{ca}$ = 0.2 [%] and variant $B$ = concrete material permissible strain parameter, i.e. $e_{ca}$ = 0.35 [%]. The load factor $\gamma_{LM1}$ for LM1 ($\gamma_{LM1}$ = 1.00 for 100 % applied LM1 at the most unfavourable position on the whole bridge) vs. the vertical deflection of the endpoint of the cantilever beam (indicated in Fig. 2) is illustrated in Fig. 6. It can be clearly seen, that (a) the reduction in the number of tendons can lead to up to 30 % of a possible quadruple loading increase in the maximum load, (b) distinguishing $e_{ca}$ does not have any dominant influence on the loadbearing behaviour in the load-carrying state and (c) a more ductile system does not emerge until 45 % of the tendons fail, where deformability increases and the LM1 load can only be doubled. The phenomenon of an increase in the maximum load capacity caused by fewer tendons is also reflected in the development of the robustness with respect to the degradation processes, as shown in Fig. 7.

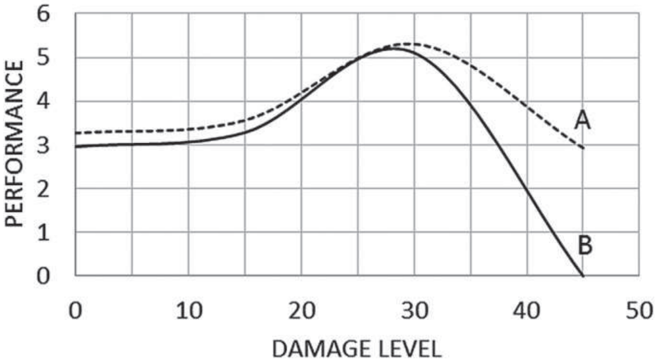


**Fig. 7.** Robustness curves for damage scenario $ds1$ for $A$ with $e_{ca}$ = 0.2 and $B$ with $e_{ca}$ = 0.35; the performance reflects the overload factor $\gamma_{LM1}$

This robustness has been computed according to Eq. (4) with an initial reliability index $\beta_{intact}$ = 6.00 extracted from a probabilistic analysis. The system performances and characteristics detected for the virgin and the degraded structure are primarily operators for predictive models (see also [10], [11]) for the compliance of the structural performance over the planned lifetime $t_L$ and the assessment of the remaining lifetime $t_R$. This phenomenon of an increase in load capacity and robustness occurs in a similar manner in damage scenarios $ds2$ and $ds3$. Damage scenario $ds2$ follows the setup of $ds1$ with the exception of statistically dependent (in terms of damage accumulation) random sampling for structure $A$ only. Such sampling schemes yield lower ultimate capacity values, as shown in Fig. 8. The third scenario ($ds3$) follows the setup of $ds2$, adding a reduction in the prestressing force to 80 % of its original value as a result of excessive creep in combination with the random removal of prestressing tendons. The qualitative robustness evaluation for structure $A$ and all three scenarios are represented by the robustness curves [11] in Fig. 9 for both the peak resistance and its associated deflection.

The simulated behaviour of various damage scenarios presented here reveals a trend that proved to be persistent in every realization of the virtual experiment. In addition, the ultimate capacity of the virgin structure shows a smaller load-carrying capacity than the system with fewer pretensioned tendons, e.g. due to the degradation processes detected. In addition, the robustness investigations on the Colle Isarco Bridge with respect to the robustness formulations of Eqs. (1) to (7) show that the probabilistic-based formulations (Eqs. (4) and (5)) are more appropriate due to the high scattering in the damage scenarios and the structural responses.

These findings are supported by the quasi semi-deterministic simulations presented in Fig. 10. In this figure, the system responses (semi-deterministic representation) for the 5 and 50 % fractile values are outlined on the basis of the stochastic input values as shown in Tables 1 and 2.

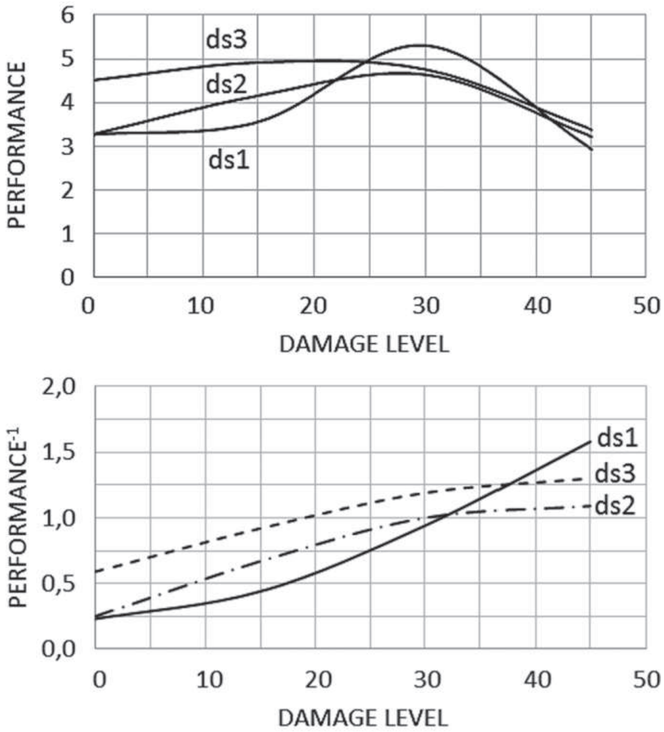


**Fig. 9.** Robustness distribution for damage scenarios *ds*1 to *ds*3

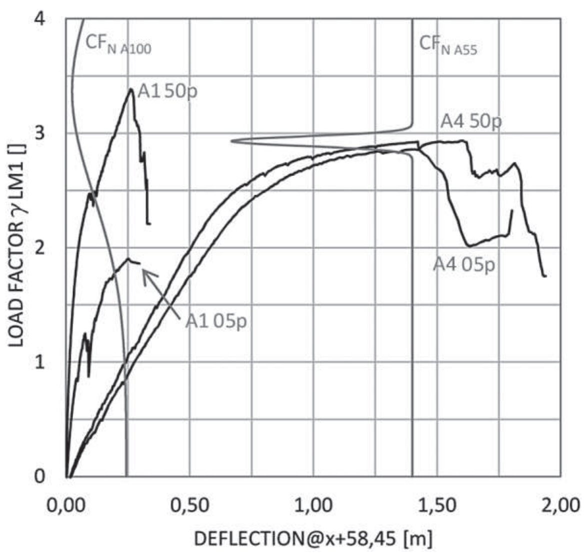


**Fig. 10.** Fractile development (50 and 5 % fractiles) of the system responses for damage scenario *ds*1 with regard to the ECOV analysis for *A*1 (virgin) and damaged (*A*4) model. Grey lines represent fitted normal distribution ($CF_{xx}$) using a relative scale.

From these processes it clearly emerges that there is a need to integrate the statistical moments as well as the density function of the system responses into the formulation of the performance indicators (which generally takes the form of a lognormal distribution), as performed in Eqs. (4) and (5).

The deterioration studies of the Colle Isarco bridge, especially the tendon failure scenarios investigated, have shown that:

(a) the load-carrying capacity of the virgin structure $\gamma_{LM1} = 2.93$ ($ds1$, $A1$) is higher than that required by the LM1 load model according to EN 1991,
(b) the maximum load-carrying capacity $\gamma_{LM1} = 5.31$ can be reached in the case of an $A3 = 30$ % failure of the tendons, which is, however, associated with an unacceptable deflection value of 1.00 m where serviceability limit states are relevant, and
(c) due to the possibility of the high tendon failure rate that may occur before any problems regarding the load-carrying capacity arise, it may be deduced that both load-carrying capacity and performance will be suitably achieved up to the end of the service life $t_L$.

Based on the inspections, a maximum deterioration rate of 10 % may be deduced for any box girder cross-section after an operating life of 30 years. However, a comprehensive set of conservation measures is scheduled within the next three years. In terms of the load-carrying capacity, it may be concluded that the structure examined exhibits sufficient capacity under all relevant damage scenarios, reflecting current and future conditions, far beyond the planned life span.

For the quantification of the performance indicators presented above with respect to robustness and redundancy, probabilistic simulation approaches were necessary to (a) obtain the statistical characteristics of the response quantities, e.g. in terms of the probability density (PDF) distribution parameters (see Table 5), and (b) obtain the required set of reliability indexes ß associated with both the initial and the damaged structural conditions, whereas the following limit state function is formulated using action $E$ and resistance $R$ models:

$$p_f = P(R - E < 0) \tag{8}$$

where the action model $E$ is represented by a deterministic value of 1, i.e. the design load. The resulting probabilities are presented together with the relevant safety indexes in Table 6. Please note that deterministic action was used to demonstrate and separate the effect of various resistance models. The conventional method would account

**Table 5.** Statistical characteristics of load factor $\gamma_{LM1}$

| Origin | *m* | COV | PDF |
|---|---|---|---|
| $R_{min} = ds1$ | 2.93 | 0.09 | lognormal |
| $R_{max} = ds3$ | 5.31 | 0.13 | lognormal |

**Table 6.** Reliability index and failure probability $p_f$ with respect to structural response and 100 % LM1 ($\gamma_{LM1} = 1.00$) load model of damage scenarios *ds*1 to *ds*3

| ULS | *m* | COV | $\beta$ | $p_f$ |
|---|---|---|---|---|
| Z ($R_{min}$,$E$) | 1.92 | 0.13 | **7.32** | 1.2e-13 |
| Z ($R_{max}$,$E$) | 4.31 | 0.16 | **6.24** | 2.1e-10 |

**Table 7.** Robustness- and redundancy-associated performance indicators for the Colle Isarco Bridge

| Name | Symbol | Eq. | Value |
|---|---|---|---|
| Redundancy Factor | $\beta_R$ | (4) | 6.77 |
| Robustness Index | $RI$ | (5) | 1749 |
| Reserve Strength Ratio | $RSR$ | (6) | 5.31 |
| Damaged Strength Ratio | $DSR$ | (7) | 2.93 |

for the uncertainty values in the action model as well. The least performing scenario $R_{min}$ in terms of mean value of 1.92 in fact has higher safety index $\beta = 7.32$ when compared with the best performing scenario $R_{max}$, with its $\beta$ value of 6.24. This means that by including the higher moment's statistics for response, we obtain the expected behaviour (i.e. more damage leading to less performance, in contrast to the evidence presented in Figs. 6 and 8). Finally, selected damage-based performance indicators for the Colle Isarco Bridge are presented in Table 7 for the most extreme scenarios of ultimate capacity, designated in the text as $R_{min}$ and $R_{max}$.

Since such indicators were designed for and are typically used to evaluate the performance of parallel systems, e.g. frame structures or suspension bridges, it is difficult to find reference values at this time for concrete structures designed as statically determinate. An analogy to parallel systems made here can only assume the deactivation of the system's mass (concrete, reinforcement) or function (prestressing).

## 4 Estimation of coefficient of variation (ECOV) approach

The ECOV method was introduced by *Cervenka* [5] to simplify the computationally intensive fully probabilistic method. In this method the coefficient of variation $V_R$ of, for example, the structural resistance is estimated using two separate non-linear analyses with mean and characteristic input values. Assuming lognormal distribution, as is typically used for structural resistance due to the prevailing multiplicative operations involved in the calculations, $V_R$ may be expressed as

$$V_R = \frac{1}{1.65} \ln\left(\frac{R_m}{R_k}\right) \tag{9}$$

where $R_m$ and $R_k$ represent mean and characteristic response quantity respectively. The global safety factor $\gamma_R$ of resistance is then estimated as

$$\gamma_R = \exp(\alpha_R \; \beta \; V_R) \tag{10}$$

where $\alpha_R$ is the sensitivity factor for resistance reliability and $\beta$ is the reliability index. This procedure complies with the principles of reliability assessment as formulated in engineering code specifications. According to Eurocode 2, typical values are 4.7 for $\beta$ (reference period of one year) and 0.8 for $\alpha_R$. Finally, the design resistance can be calculated as

$$R_d = \frac{R_m}{\gamma_R} \tag{11}$$

Such approximations improve the confidence of the EN 1992-1-1 estimation while reducing the computational input of the fully probabilistic approach. As a consequence, the safety of resistance can be formulated according to Cervenka [5] in objective and rational terms. In Fig. 10, the fractile development alternatives required for the ECOV analysis (50 and 5 % fractiles) of the system responses are shown for damage scenarios $ds1$: $A1$ and $A4$. This resulted in coefficients of variation $V_{R,A1} = 35$ % and $V_{R,A4} = 1.5$ %. The application of these variation coefficients to the global safety factor approach of resistance results in $\gamma_{R,A1} = 2.95$ and $\gamma_{R,A4} = 1.05$ and, finally, in the design resistance in terms of the LM1 overload factor, $R_{d,A1} = 1.14$ and $R_{d,A4} = 2.80$.

The respective load–deflection diagrams are depicted in Fig. 10 together with PDFs fitted to two fixed points. Note that the large difference in variance is clearly responsible for the smaller design resistance of the virgin structure. In addition, such approximation methods in combination with complex structural models have to be treated with caution, especially where sensitive asymmetrical distributions are considered. In many instances, physically insignificant modifications of the computational model lead to performance shifts on a logarithmic scale.

## 5 New strategy for complex engineering structures

**What have we learned?** There are already promising approaches for assessing the system performance which can clearly differ from the individual component assessment. The system performance concepts, which are based, for example, on robustness and redundancy, require (a) probabilistic methods for the incorporation of uncertainties in the input data and the structural response, and (b) the definition of clearly specified criteria associated with robust or non-robust systems.

**How can the system performance concepts generally be applied?** The global safety factor concept ECOV, which is based on the distribution of two fractiles of the structural response provides (a) the possibility to define global safety factors for general systems, and (b) inputs for the robustness and redundancy assessment of a system. Therefore, the ECOV approach combined with robustness and redundancy methods can be considered as a logical and simple assessment procedure.

## 6 Conclusions

The objective of the current paper is to quantify the effects of relevant, combined deterioration mechanisms and mechanical actions and to compare these effects with the behaviour of an intact and current state system.

1. Due to the uncertainties in environmental loading, mechanical degradation processes and inspection records, a parameter study with reduced critical elements has been considered as a suitable procedure for assessing reliability and remaining lifetime.
2. The reliability assessment is usually related to the critical member of a system and not the whole system. Ro-

bustness and redundancy approaches are therefore considered to be more appropriate because they take into account the redistribution ability of the system. This study examines the feasibility of several formulations with respect to robustness and redundancy.
3. The cantilever bridge case study demonstrates that robustness is not a monotonic function but can increase in the case of certain damage scenarios.
4. Nevertheless, the study also shows that robustness can be an appropriate indicator for bridge owners who wish to evaluate the fitness of their structures.
5. Additionally, the performance indicators were compared to the semi-deterministic approximation method, the global safety factor. The development was in agreement with the deterministic performance indicators such as Damaged Strength Ratio and Reserve Strength Ratio.

The investigation of the Colle Isarco Bridge shows that in terms of design and assessment, bridges may exhibit a significant increase in loading capacity when system failure rather than element failure is considered. From this perspective, the bridge analysed sustains all damage scenarios that were developed, maintaining the operational and safety requirements, including realistic data from in situ measurements and subsequent identification of remaining material parameters. The framework presented can be applied to a variety of engineering structures beyond the deemed-to-satisfy concept, such as bridges, water reservoirs, dams, etc.

### Acknowledgements

This research was conducted with the financial support of the Austrian Research Agency FFG and the "Zentrum für Innovation und Technologie GmbH – ZIT" within the scope of the "Comprehensive Infrastructure Life-Cycle Assessment" (CILIA) and "Monitoringbasiertes Softwareprodukt für die Lebenszeitbewertung ermüdungsgefährdeter Betonstrukturen" (MLEB) projects. The current research was partly supported financially by the Austrian Science Funds FWF as part of the Doctoral Programme on Water Resource Systems (DK-plus W1219-N22).

### References

1. *Ahrens, M. A., Strauss, A., Bergmeister, K., Mark, P., Stangenberg, F.*: Lebensdauerorientierter Entwurf, Konstruktion, Nachrechnung. In: Bergmeister, *K., Fingerloos, F., Wörner, J.-D.*: Beton-Kalender 2013, Lebensdauer und Instandsetzung – Brandschutz Betonkalender, Ernst & Sohn, Berlin, 2013.
2. *Anitori, G., Casas, J. R., Ghosn, M.*: Redundancy of Highway Bridge Decks. Bridge Maintenance, Safety, Management, Resilience and Sustainability: Proceedings of the Sixth International IABMAS Conference, Stresa, Lake Maggiore, Italy, 8–12 July 2012.
3. *Biondini, F., Frangopol, D. M.*: Lifetime Structural Robustness of Concrete Bridge Piers under Corrosion. Bridge Maintenance, Safety, Management, Resilience and Sustainability: Proceedings of the Sixth International IABMAS Conference, Stresa, Lake Maggiore, Italy, 8–12 July 2012.
4. *Bogath, J.*: Verkehrslastmodelle für Strassenbrücken. Beitrag zur Entwicklung eines probalistischen Verkehrslastmodells. Dissertation, Universität für Bodenkultur, Vienna, 1997.
5. *Cervenka, V.*: Reliability-Based Non-Linear Analysis According to *fib* Model Code 2010. Structural Concrete, 14, No. 1 (2013), pp. 19–28.
6. *Cervenka, V., Cervenka, J.*: Verification of Bridge Repair Assisted by Numerical Simulation. Concrete repair, rehabilitation and retrofitting International Conference; 405–406, ISBN: 9780415899529, 2012.
7. *Decò, A., Bocchini, P., Frangopol, D. M.*: A Probabilistic Approach for the Prediction of Seismic Resilience of Bridges. Earthquake Engineering and Structural Dynamics, 42, No. 10 (2013), pp. 1469–1487.
8. *Frangopol, D. M., Curley, J. P.*: Effects of Damage and Redundancy on Structural Reliability. Journal of Structural Engineering, 113, No. 7 (1987), pp. 1533–1549.
9. *Ghosn, M., Moses, F.*: NCHRP Report 406, Redundancy in Highway Bridge Superstructures. Transportation Research Board, National Research Council, National Academy Press, Washington, D.C., 1998.
10. *Ghosn, M., Frangopol, D. M., McAllister, T. P., Shah, M., Diniz, S., Biondini, F., Catbas, N., Strauss, A., Liu, Y., Zhao, Z. L.*: Part I: Reliability-based structural performance indicators: Development and implementation for elements SEI-ASCE Technical Council on Life-Cycle Performance, Safety, Reliability and Risk of Structural Systems, Task 2 Group: Reliability Based Structural System Performance Indicators, 2013a.
11. *Ghosn, M., Duenas-Osorio, L., Frangopol, D. M., Arangio, S., Bontempi, F., McAllister, T. P., Bocchini, P., Shah, M., Akiyama, M., Biondini, F., Hernandez., S.*: Part II: Reliability-based structural performance indicators for structural systems and networks SEI-ASCE Technical Council on Life-Cycle Performance, Safety, Reliability and Risk of Structural Systems, Task 2 Group: Reliability Based Structural System Performance Indicators, 2013b.
12. *Jendele, L., Cervenka, J.*: On the Solution of Multi-Point Constraints – Application to FE Analysis of Reinforced Concrete Structures. Computers and Structures, 87, No. 15–16 (2009), pp. 970–980.
13. *Joris, J. P.*: Bundesamt für Straßen der Schweizerischen Eidgenossenschaft, Bereich Kunstbauten, Bern, 2002.
14. *Maes, M. A., Fritzsons, K. E., Glowienka, S.*: Structural Robustness in the Light of Risk and Consequence Analysis. Structural Engineering International: Journal of the International Association for Bridge & Structural Engineering (IABSE), 16, No. 2 (2006), pp. 101–107.
15. *Matthews, S., Bigaj-van Vliet, A., Ueda, T.*: *fib* Model Code 2010 – Chapter 9: Conservation of concrete structures. 3rd International Conference on Concrete Repair, Rehabilitation and Retrofitting, ICCRRR-3, 3-5 September 2012, Cape Town, South Africa, Edited by Pilate Moyo, CRC Press 2012, Print ISBN: 978-0-415-89952-9.
16. *Melchers, R. E.*: Structural Reliability Analysis und Prediction. Wiley, Chichester/New York/Brisbane/Toronto, 1999.
17. *Novák, D., Vořechovský, M., Lehký, D., Bergmeister, K., Pukl, R., Červenka, V.*: Stochastic Nonlinear Analysis of Concrete Structures – Part I: From Simulation of Experiment and Parameter Identification to Reliability Assessment, 10th, International conference on applications of statistics and probability in civil engineering; ICASP 10; 325–326, 2007.
18. *Podroužek, J., Teplý, B.*: Modelling of chloride Transport in concrete by cellular automata. Engineering Mechanics, vol. 15, No. 3, pp. 213–222, 2008.
19. *Pryl, D., Cervenka, J., Pukl, R.*: Material Model for Finite Element Modelling of Fatigue Crack Growth in Concrete. Procedia Engineering, Volume 2, Issue 1, April 2010, Pages 203–212.

20. *Pukl, R., Červenka, V., Červenka, J., Novák, D.*: Computer Simulation of Concrete Bridges. Proc. IABMAS 2012, Stresa, Italy, 08. – 12. 07. 2012, ISBN 978-0-41562124-3, pp. 684.
21. *Pukl, R., Červenka, V., Novák, D., Teplý, B., Strauss, A., Bergmeister, K.*: Life Cycle Reliability Assessment Based on Advanced Structural Modeling – Nonlinear FEM. Third International Conference on Bridge Maintenance, Safety and Management, Porto, 16 – 19 July 2006.
22. *Rubin, H.*: Second Order Theory for Beam and Arch Structures under Hydrostatic Pressure. Theorie II. Ordnung für Stabwerke und Stabbogen unter Hydrostatischem Druck, Bautechnik, 79, No. 6 (2002), pp. 384–395.
23. *Santa, U., Bergmeister, K., Strauss, A.*: Structural Monitoring of Concrete Bridges. Bauwerksüberwachung der Autobahnbrücke Gossensass, 99, No. 12 (2004), pp. 975–984.
24. *Schneider, J.*: Introduction to Safety and Reliability of Structures. Structural engineering Documents, 1997.
25. *Schneider, J.*: Sicherheit und Zuverlässigkeit, vol. 1, vdf, 1994.
26. *Spaethe, G.*: Die Sicherheit Tragender Baukonstruktionen. Springer, Vienna, 1992.
27. *Stewart, M. G., Mullard, J. A.*: Spatial Time-Dependent Reliability Analysis of Corrosion Damage and the Timing of First Repair for RC Structures. Engineering Structures, 29, No. 7 (2007), pp. 1457–1464.
28. *Strauss, A., Bergmeister, K., Novák, D., Lehký, D.*: Probabilistic Response Identification and Monitoring of Concrete Structures. Stochastische Parameteridentifikation bei Konstruktionsbeton für die Betonerhaltung, Beton- und Stahlbetonbau, 99, No. 12 (2004), pp. 967–974.
29. *Strauss, A., Bergmeister, K., Wendner, R., Hoffmann, S.*: System- und Schadensidentifikation von Betonstrukturen. In: Betonkalender 2009, eds. *Bergmeister, K., Wörner, J. D.*, Ernst & Sohn, Berlin, 2009, pp. 55–125.
30. *Strauss, A., Frangopol, D. M., Bergmeister, K.*: Assessment of Existing Structures Based on Identification. Journal of Structural Engineering, 136, No. 1 (2010), pp. 86–97.
31. *Strauss, A., Wendner, R., Bergmeister, K., Costa, C.*: Numerically and Experimentally Based Reliability Assessment of a Concrete Bridge Subjected to Chloride-Induced Deterioration. Journal of Infrastructure Systems, 19, No. 2 (2013), pp. 166–175.
32. *Teplý, B., Vořechovská, D.*: Reinforcement Corrosion: Limit States, Reliability and Modelling. Journal of Advanced Concrete Technology, 10, No. 11 (2012), pp. 353–362.
33. *Zienkiewicz, O. C., Taylor, R. L., Zhu, J. Z.*: The Finite Element Method: Its Basis and Fundamentals, 6th ed., Elsevier, 2005.
34. *Gouverneur, D., Caspeele, R., Taerwe, L.*: Experimental investigation of the load-displacement behaviour under tensile membrane action in a restrained reinforced concrete slab strip. Engineering Structures, Vol. 49 (2013), pp. 1007–1016.
35. *Gouverneur, D., Caspeele, R., Taerwe, L.*: Effect of reinforcement curtailment on deflections, strain and crack development in RC slabs under catenary action. Magazine of Concrete Research, Vol. 65, No. 22, pp. 1336–1347 (in press).
36. *Strauss A., Frangopol, D. M., Kim, S.* (2008), Use of monitoring extreme data for the performance prediction of structures: Bayesian updating. Engineering Structures, 30. 3654–3666.
37. *Frangopol, D. M., Strauss, A., Kim, S.* (2008), Use of monitoring extreme data for the performance prediction of structures: General approach. Engineering Structures, 30. 3644–3653.



Jan Podroužek
PhD candidate, Doctoral Programme on Water Resource Systems, Centre for Water Resource Systems, Vienna University of Technology, Peter-Jordanstr. 82, Vienna, A-1190, Austria
E-mail: podrouzek@waterresources.at



Alfred Strauss
Associate Professor, Department of Civil Engineering & Natural Hazards, University of Natural Resources & Life Sciences, Peter-Jordanstr. 82, Vienna, A-1190, Austria
E-mail: alfred.strauss@boku.ac.at



Konrad Bergmeister
Professor, Department of Civil Engineering & Natural Hazards, University of Natural Resources & Life Sciences, Peter-Jordanstr. 82, Vienna, A-1190, Austria
E-mail: konrad.bergmeister@boku.ac.at

## 6. Conclusion

The studies presented as part of the Doctoral Programme on Water Resource Systems have offered an evaluative perspective on an important aspect of quantified environmental hazards, the computational analysis of randomness and feasible solution strategies.

Of particular interest were the statistical characterizations of stochastic transient structural loads, heterogeneity, combined environmental effects and deterioration mechanisms, all challenging and open research questions. On selected case studies from the fields of structural mechanics and water resources, new concepts were elaborated and verified through numerous test cases, including non-traditional numerical schemes and involved nested high-dimensional Monte Carlo simulations, i.e. MC simulation of MC simulations etc. The consequential parsing revealed new features that again required more simulations to check them which in turn revealed new features that had to be validated etc. Maintaining a single direction in the development process proved to be another challenging task when subjected to constantly growing set of evidence from digital simulations and the author has to admit that not infrequently has found himself wondering in loops or around unrelated themes.

Since almost anything can be formulated within an MC framework, it easily creates computational demand. Often, such demand is beyond the scope of available capacity, and, more importantly, such demand cannot be justified if effective reduction schemes are available. And computational analysis of randomness together with uncertainty quantification rarely cannot benefit from repeated MC trials. By considering current and newly emerging performance indicators for engineered systems subjected to ever changing environment, the demand and motivation should follow.

The issue of seismic risk was covered in the second chapter, mostly in relation to structural dynamics, where a novel strategy was introduced enabling the identification of critical samples of stochastic oscillatory processes from a finite set with respect to the response of given mechanical model. From a design point of view, it is essential to identify what particular realization of such a process has critical impact on the structural response. Any non-linear dynamical system has a different and unique response to various realizations of probabilistically different ground motion events [Clough & Penzien 1975]. Consequently, for Monte-Carlo-based structural reliability considerations, a very large number of realizations of the stochastic load must be considered and analyzed, making the task computationally unfeasible for realistic failure probabilities. Up to date of submitting the chapter 2 and 3 papers, no sampling technique was capable of reducing such probabilistic formulation with the exception of the proposed STS method, according to authors knowledge.

The possibilities of more general soft-computing approach were examined in the following chapter, resulting in software development for a fast prescreen of Monte Carlo transient samples and consequent importance sampling strategy. An important consequence is that the proposed STS strategy moves the advantages of a fully probabilistic approach within the context of dynamical systems one step closer to engineering practitioners, motivated by the ever-growing demand for performance-based design. Beyond the engineering community, the proposed STS strategy may prove to be a useful technique in the context of environmental sciences, such as water resources, addressing analogous problems such as identifying critical precipitation events.

Regarding further research, among the key objective would be a general formulation of a relationship between the first passage probabilities accuracy and the STS training sample size. Despite author’s intention, such effort requires extensive processing capabilities if to be treated by MC, or more analytical skills.

Another interesting aspect would be the reconstruction of a correlation structure between the STS quantified feature and the critical response variable. The actual distribution asymmetry makes the use of current bivariate models ineffective while the kernel distribution has too many parameters for an MC based parameters fit.

In chapter 4 the discussion concerned the difficulty of describing possibilistic set of deteriorations states, a formulation required for the quantification of damage-based performance indicators and consequent optimal maintenance planning. The investigations showed, among others, that structures may exhibit a significant increase in loading capacity when system failure rather than element failure is considered and that non-monotonous robustness may have an unexpected course. The simulations also revealed the importance of considering the so called solver noise, a non-physical solution artifact that can significantly affect the statistical response, when compared to the effect of inherent variability of e.g. material properties.

Although the several newly proposed concepts from the probabilistic context of infrastructure safety have upgraded the selection of available solution strategies, the author would like to express a more general statement with regards to theirs transfer. Still, rather a long distance remains between arousing interest and confidence of the professional public, and the current state, not only with respect to black-box type of approaches, although efficient and often more transparent when compared to established top-down methods.

Nevertheless, classical analytical approaches should always remain among the first to consider verification tools, and in many instances, also entirely adequate.

## References

Ahrens, M.A., Strauss, A., Bergmeister, K., Mark, P., and Stangenberg, F. "Lebensdauerorientierter Entwurf, Konstruktion, Nachrechnung." In In Bergmeister, Konrad / Fingerloos, Frank / Wörner, Johann-Dietrich; Beton-Kalender 2013, Lebensdauer und Instandsetzung – Brandschutz Betonkalender. Berlin: Ernst und Sohn, 2013.

Ang, A.H., and Tang, W.H. Probability Concepts in Engineering Planning, John Wiley, 2nd Edition, 2007.

Anitori, G., Casas, J. R., and Ghosn, M. "Redundancy of Highway Bridge Decks" Bridge Maintenance, Safety, Management, Resilience and Sustainability, Proceedings of the Sixth International IABMAS Conference, Stresa, Lake Maggiore, Italy, Edited by Fabio Biondini Dan M . Frangopol, CRC Press 2012, pp 2252–2259, Print ISBN: 978-0-415-62124-3, 2012.

Bay, H., A. Ess, T. Tuytelaars and L van Gool, "SURF: Speeded Up Robust Features", Computer Vision and Image Understanding (CVIU), Vol. 110, No. 3, pp. 346-359, 2008.

Bamer, F., and Bucher, Ch. "Application of the proper orthogonal decomposition for linear and nonlinear structures under transient excitations", Acta Mechanica 223, 2549-2563, 2012.

Barbato, M., and Conte, J.P. "Structural Reliability Applications of Nonstationary Spectral Characteristics", Journal of Engineering Mechanics, ASCE, pp. 371-382, 2011.

Biondini, F., and Frangopol, D. M. "Lifetime Structural Robustness of Concrete Bridge Piers under Corrosion." Bridge Maintenance, Safety, Management, Resilience and Sustainability, Proceedings of the Sixth International IABMAS Conference, Stresa, Lake Maggiore, Italy, Edited by Fabio Biondini Dan M . Frangopol, CRC Press 2012, pp 2252–2259, Print ISBN: 978-0-415-62124-3, 2012.

Bogath, J. „Verkehrslastmodelle für Strassenbrücken Beitrag zur Entwicklung eines probalistischen Verkehrslastmodells“, Dissertation Universität für Bodenkultur, Wien, 1997.

Bucher, Ch. "Optimal probabilistic design of friction-based seismic isolation devices, Safety, Reliability and Risk of Structures", Infrastructures and Engineering Systems – Furuta, Frangopol & Shinozuka (eds), Taylor & Francis Group, London, ISBN 978-0-415-47557-0, 2010.

Bucher, Ch. Computational analysis of randomness in structural mechanics. Ed. by D. M. Frangopol. Structures and Infrastructures Book Series, Vol. 3., London: Taylor & Francis, 2009.

Cervenka, V. "Reliability-Based Non-Linear Analysis According to Fib Model Code 2010." Structural Concrete 14, no. 1, 19-28, 2013.

Decò, A., Bocchini, P. and Frangopol, D. M. "A Probabilistic Approach for the Prediction of Seismic Resilience of Bridges." Earthquake Engineering and Structural Dynamics 42, no. 10, 1469-87, 2013.

Clough, R.W. and Penzien, J. Dynamics of structures, McGraw-Hill, 1975.

Deodatis, G., "Non-stationary stochastic vector processes: seismic ground motion applications", Probabilistic Engineering Mechanics, Vol. 11, Issue 3, pp. 149-167, 1996.

Deodatis, G. and Shinozuka, M. "Auto-Regressive Model for Non-Stationary Stochastic Processes", Journal of Engineering Mechanics, ASCE, Vol. 114, No.11, pp. 1995-2012, 1988.

Drenick, R.F. "The critical excitation of nonlinear systems", J. Appl. Mech., pp. 333-336, 1977.

Foster I, Kesselman C and Tuecke S. "The anatomy of the Grid: Enabling scalable virtual organizations." International Journal of High Performance Computing Applications; 15(2):200–222, 2001.

Frangopol, D. and Curley, J.P. "Effects of Damage and Redundancy on Structural Reliability." Journal of Structural Engineering 113, no. 7: 1533-49, 1987.

Ghosn, M., and F. Moses. Nchrp Report 406, Redundancy in Highway Bridge Superstructures. Washington. DC: Transportation Research Board---National Research Council, National Academy Press, 1998.

Ghosn, M., Frangopol, D., McAllister, T. P., Shah, M., Diniz, S., Biondini, F., Catbas, N., Strauss, A., Liu; Y. and Zhao, Z. L. "Part I Reliability-based structural performance indicators: Development and implementation for elements SEI-ASCE Technical Council on Life-Cycle Performance, Safety, Reliability and Risk of Structural Systems Task 2 Group: Reliability Based Structural System Performance Indicators.“ 2013.

Harvey, J. and Bencala, K. "The effect of streambed topography on surface-subsurface water exchange in mountain catchments", Water Resources Research, 29, 8998, 1993.

Jendele, L., and J. Červenka. "On the Solution of Multi-Point Constraints - Application to Fe Analysis of Reinforced Concrete Structures." Computers and Structures 87, no. 15-16, 970-80, 2009.

Joris, J.P. and Bern, V. Bundesamt für Straßen der Schweizerischen Eidgenossenschaft - Bereich Kunstbauten, 2002.

Kahn, H. and Marschall, A.W. "Methods of Reducing Sample Size in Monte Carlo Computations." Journal of the Operations Research Society of America, Vol. 1, No. 5, pp.263-278, 1953.

Kahn, H. Stochastic (Monte Carlo) Attenuation Analysis, Rand Corporation, 1949.

Der Kiureghian, A. "The geometry of random vibrations and solutions by FORM and SORM." Probabilistic Engineering Mechanics 15.1, pp. 81 –90, 2000.

Der Kiureghian, A. and Liu, P-L. "Structural Reliability under Incomplete Probability Information" J. Eng. Mech., 112(1),85-104, 1986.

Macke, M., and Bucher, Ch. "Importance sampling for randomly excited dynamical systems", Journal of Sound and Vibrations 268, pp. 269-290, 2003.

Maes, M. A., Fritzsons, K. E. and Glowienka, S. "Structural Robustness in the Light of Risk and Consequence Analysis." Structural Engineering International:

Journal of the International Association for Bridge and Structural Engineering (IABSE) 16, no. 2, 101-07, 2006.

Marano, G.C. and Quaranta G. "A new possibilistic reliability index definition" Acta Mechanica, March 2010, Volume 210, issue 3-4, pp 291-303.

Matthews, S., A. Bigaj-van Vliet, Ueda, T. fib Model Code 2010 – Chapter 9: Conservation of concrete structures. Structural Concrete: 2013.

Melchers, R.E. Structural Reliability Analysis Und Prediction. Chichester - New York - Brisbane - Toronto: Wiley, 1999.

Moustafa, A., "Damage-Based Design Earthquake Loads for Single-Degree-Of-Freedom Inelastic Structures", Journal of Structural Engineering, ASCE, pp. 456-467, 2011.

Mwakanyamale, K., Slater, L., Day-Lewis, F., Elwaseif, M., and Johnson, C. "Spatially variable stage-driven groundwater-surface water interaction inferred from time-frequency analysis of distributed temperature sensing data", Geophysical Research Letters, 39, doi:10.1029/2011GL050824, 2012.

Novák, D., Vořechovský, M., Lehký, D., Bergmeister, K., Pukl, R. and Červenka, V. "Stochastic Nonlinear Analysis of Concrete Structures - Part I: From Simulation of Experiment and Parameter Identification to Reliability Assessment." 2007.

Novak, D., Strauss, A., Bergmeister, K., Hoffman, V. and Pukl, R. "Advanced life-cycle analysis of existing concrete bridges", Journal of Materials in Civil Engineering, 20(1), pp. 9-19, 2008.

Payn, R. A., Gooseff, M. N., McGlynn, B. L., Bencala, K. E., and Wondzell, S. M. "Channel water balance and exchange with subsurface flow along a mountain headwater stream in Montana, United States", Water Resources Research, 45, doi: 10.1029/2008WR007644, 2009.

Podroužek, J., and Teplý B. Modelling of chloride Transport in concrete by cellular automata. Engineering Mechanics, Vol. 15, No.3, p. 213-222, 2008.

Priestley, M.B. Non linear and non stationary time series analysis, Academic Press, 237 p, 1988.

Priestley, M. B. "Evolutionary Spectra and Non-Stationary Processes", Journal of the Royal Statistical Society, Series B (Methodological), Vol. 27, No. 2, pp. 204-237, 1965.

Pryl, D., Cervenka, J. and Pukl, R. "Material Model for Finite Element Modelling of Fatigue Crack Growth in Concrete." 2010.

Pukl, R., Červenka, V., Červenka, J. and Novák, D. "Computer Simulation of Concrete Bridges." 2012.

Pukl, R., Červenka, V., Novák, D., Teplý, B., Strauss, A. and Bergmeister, K. "Life Cycle Reliability Assessment Based on Advanced Structural Modeling - Nonlinear Fem." 2006.

R Development Core Team. R: A Language and Environment for Statistical Computing, http://www.R-project.org/, 2011.

Rubin, H. "Second Order Theory for Beam and Arch Structures under Hydrostatic Pressurel." Theorie II. Ordnung für Stabwerke und Stabbogen unter Hydrostatischem Druck 79, no. 6, 384-95, 2002.

Rubinstein, A. Modeling bounded rationality. MIT Press. ISBN 0-585-05347-2, 1998.

Santa, U., Bergmeister, K. and Strauss, A. "Structural Monitoring of Concrete Bridges." Bauwerksüberwachung der Autobahnbrücke Gossensaß 99, no. 12, 975-84, 2004.

Shinozuka, M. and Deodatis, G. "Simulation of Stochastic Processes by Spectral Representation", Appl. Mech. Rev. 44, 191, DOI:10.1115/1.3119501, 1991.

Schaffer, J. Deterministic Chance? Br J Philos Sci 58 (2): 113-140, doi:10.1093/bjps/axm002, 2007.

Schneider, J. "Introduction to Safety and Reliability of Structures." Structural engineering Documents, 1997.

Schneider, Jörg. Sicherheit und Zuverlässigkeit. Vol. 1: vdf, 1994.

Spaethe, G. Die Sicherheit tragender Baukonstruktionen.  Wien: Springer, 1992.

Steineck, R.C. and Clausius C (eds.). "Origins as futures in the time plays of J.B. Priestley" in Origins and Futures: Time inflected and Reflected. BRILL, ISBN 9004252002, 2013.

Stewart, M. G. and Mullard J. A.. "Spatial Time-Dependent Reliability Analysis of Corrosion Damage and the Timing of First Repair for Rc Structures." Engineering Structures 29, no. 7, 1457-64, 2007.

Strauss, A., Bergmeister, K., Novák, D. and Lehký, D. "Probabilistic Response Identification and Monitoring of Concrete Structures." Stochastische Parameteridentifikation bei Konstruktionsbeton für die Betonerhaltung 99, no. 12, 967-74, 2004.

Strauss, A., Bergmeister, K., Pukl, R., Červenka, V. and Novák, D. "Sara - a Tool within Life Span Analysis of Concrete Structures." 2003.

Strauss, A., Bergmeister, K., Wendner, R., and Hoffmann, S. "System- und Schadensidentifikation von Betonstrukturen." In Betonkalender 2009, edited by K. Bergmeister and J.D. Wörner. 55-125. Berlin: Ernst und Sohn, 2009.

Strauss, A., Frangopol, D. M. and Bergmeister, K. "Assessment of Existing Structures Based on Identification." Journal of Structural Engineering 136, no. 1,  86-97, 2010.

Strauss, A., Wendner, R., Bergmeister, K. and Costa, C. "Numerically and Experimentally Based Reliability Assessment of a Concrete Bridge Subjected to Chloride-Induced Deterioration." Journal of Infrastructure Systems 19, no. 2 166-75, 2013.

Takewaki, I. "Probabilistic Critical Excitation Method for Earthquake Energy Input Rate", Journal of Engineering Mechanics, ASCE, pp. 990-1000, 2006.

Teplý, B. and Vořechovská, D. "Reinforcement Corrosion: Limit States, Reliability and Modelling." Journal of Advanced Concrete Technology 10, no. 11,  353-62, 2012.

Tezcan, J., Nonlinear System Response to Nonstationary Input Processes using Harmonic Wavelets, A thesis submitted in partial fulfillment of the requirements for the degree Doctor of Philosophy, Rice University, Houston, Texas, 2005.

Zabloudil, J. (ed.) Forschungsprojekte am Vienna Scientific Cluster: Vienna Scientific Cluster, http://vsc.ac.at/about-vsc/publications/, 2012.

Wolfram Mathematica Documentation Center, ref/WaveletScalogram, 2011.

Zienkiewicz, O.C., Taylor, R.L. and Zhu, J.Z. "The Finite Element Method: Its Basis and Fundamentals." Sixth edition, Elsevier, 2005.

**Appendix A. The code**

In sake of reproducibility of the main ideas as published in chapters 2 and 3, the essential computational environment is presented here. As a development platform for initial identification experiments and rapid prototyping of complex model scenarios was chosen *Mathematica* [© 2014 Wolfram], a commercial computer algebra system. Although this task could have been implemented in a language like PERL, C/Fortran, etc., the choice made was due to minimizing the learning curve slope and avoiding the use of different packages from many users and developers. However, during the brute-force verification period, which consisted of a large number of repeated Monte Carlo trials, the computational performance requirements, including stability, led to the choice of *SLangTNG* [© 2007 - 2014 Vienna University of Technology], a free interpreted scripting language (BSD-style licenses) based on *Lua* [© 1994 – 2014 Lua.org]. Here, the proposed identification method was rewritten and optimized for minimal computational time requirement.

Scope of this appendix is to demonstrate the functionality of the proposed method, providing a comprehensive toolbox of algorithms in the *Mathematica* code.

The input consists of

a) particular stochastic process generator, reproducing in this case the characteristics of the 1964 Niigata earthquake by means of non-stationary ground acceleration records. Instead of using a generator, another option is to load a given set of stochastic processes already available to the user.

b) particular solver module or a connection to external code, in this case a non-linear mechanical oscillator on a seismic isolation device (friction pendulum system). Due to the limited scope of this appendix, the code for realistic example of mechanical model which consists of thousands of degrees of freedom or its abstract reduction (e.g. POD) will not be shown here.

c) 3 parameters to define the full sample size, training sample size and identification confidence.

```
(*-- STS v 6.3 ©2011-2014, Jan Podrouzek, TU Wien --*)
(*-- front-end mathematica notebook ----------------*)
(*-- test case for identification run --------------*)
(*-- for comments and feedback please refer to -----*)
(*-- podrouzekj@gmail.com --------------------------*)

(*-- input definition ------------------------------*)

(* a: set of artificially generated realizations
   of ground motion time histories generated
   according to e.g. "Niigata" module *)

NiigatoGen[] := Module[{
     a1 = 0.68,
     a2 = 1 / 4,
     σ = 100,
     ωu = 128,
     Nn = 1024,
     dt = 0.01,
     nn = 2000,
     Δω, Φ},
   tp[t_] := t - 4.5;
   ωg[t_] :=
    {  15.56                                       0 ≤ t ≤ 4.5
       27.12 tp[t]^3 - 40.68 tp[t]^2 + 15.56     4.5 ≤ t ≤ 5.5 ;
       2.0                                             t > 5.5
   ξg[t_] :=
    {  0.64                                        0 ≤ t ≤ 4.5
       1.25 tp[t]^3 - 1.875 tp[t]^2 + 0.64       4.5 ≤ t ≤ 5.5 ;
       0.015                                           t > 5.5
   ωf[t_] := 0.1 ωg[t];
   ξf[t_] := ξg[t];
   A[t_] := a1 t Exp[-a2 t];
   S0[t_] := σ^2 / (π ωg[t] (2 ξg[t] + 1/(2 ξg[t])));
```

```
S[ω_, t_] := S0[t] ((1 + 4 ξg[t]^2 (ω/ωg[t])^2) / ((1 - (ω/ωg[t])^2)^2 + 4 ξg[t]^2 (ω/ωg[t])^2)) *
    (((ω/ωf[t])^4) / ((1 - (ω/ωf[t])^2)^2 + 4 ξf[t]^2 (ω/ωf[t])^2));
ωn[n_] := n Δω;
Δω = ωu/Nn;
Φ = RandomReal[{0, 2 π}, Nn];
f[t_] :=
  Sqrt[2] Sum[Sqrt[2 A[t]^2 S[ωn[n], t] Δω]
     Cos[ωn[n] t + Φ[[n + 1]]], {n, 0, Nn - 1}];

Return[Table[{ t, f[t ]}, {t, 0, nn dt, dt}]]
];
```

```
(* b: solver for mechanical model represented by
  e.g. simple nonlinear oscillator containing
  friction pendulum system *)

FPSxNDSolve[quake_] := Module[{
    m1 = 79 770,  (* kg *)
    m0 = 6080,    (* kg *)
    G = 7886,     (* kN *)
    k00 = 2629,  (* kN/m *)
    k0 = 42 372, (* kN/m *)
    k1 = 62 500, (* kN/m *)
    micro = 0.08,
    s, a, eqns, BMsolUnDamped,
    ret},
   s = G * micro;
   a = Interpolation[quake];
   eqns = {
     y1'[t] == Piecewise[{
         {0, Abs[k0 (y2[t] - y1[t])] < s},
         {0, k0 (y2[t] - y1[t]) == s && y3[t] < 0},
         {0, k0 (y2[t] - y1[t]) == -s && y3[t] > 0}},
       y3[t]],
     y2'[t] == y3[t],
     y3'[t] ==
      -a[t] - (k00 y2[t] + (k0 + k1) y2[t] - k1 y1[t]) / m0,
     y4'[t] == y5[t],
     y5'[t] == -a[t] - (k1 y4[t] - k1 y2[t]) / m1};
   BMsolUnDamped =
    NDSolve[{eqns, y1[0] == y2[0] == y3[0] == y4[0] ==
       y5[0] == 0}, {y1, y2, y3, y4, y5}, {t, 0, 19.95},
     Method → {StiffnessSwitching,
       Method → {ExplicitRungeKutta, Automatic}},
     AccuracyGoal → 5, PrecisionGoal → 4];
   ret =
    Table[
     {t,
      0.001 Evaluate[
        First[{y4[t]} /. BMsolUnDamped[[1]]]]},
     {t, 0, 19, 0.01}];
   Return[ret];
```

```
(* c: parameters *)
fsSize = 10^6;  (* Full set size *)
tsSize = 100;   (* Training set size *)
m = 10;         (* Confidence parameter *)


(*-- essential identification steps x1 to x8 -------*)

(* create 10^6 artificial records of Niigata
 earthquake *)
x1a = ParallelTable[NiigatoGen[], {n, 1, fsSize}];

x1b = Length[x1a];
x1c = RandomSample[Range[x1b], tsSize];

(* create 100 randomly sampled training set of x1a *)
x1d = ParallelTable[x1a[[x1c[[n]]]], {n, 1, tsSize}];

(* create a response vector of the solved training
 set *)
x2a = ParallelTable[Max[Abs[FPSxNDSolve[x1d[[n]]]]],
   {n, 1, tsSize}];

(* compute the integer of 5% training set size *)
x3a = IntegerPart[0.05 * tsSize];

(* create two sets with earthquake record indexes
 according to 5% maximum and minimum of the ranked
 training response vector *)
x3b = Table[{Position[x2a, RankedMax[x2a, k]][[1, 1]],
    RankedMax[x2a, k]}, {k, 1, x3a}];
x3c = Table[{Position[x2a, RankedMin[x2a, k]][[1, 1]],
    RankedMin[x2a, k]}, {k, 1, x3a}];
```

```
(* graphical transform of a part of a stochastic
 process (first 1200 records) by the
 ContinousWaveletTransform function using as
 argument the interpolated function of particular
 ground motion record *)
WSgram[qq_] := Module[{ifun, quake, cwd, img, maxmat},
   ifun = Interpolation[qq[[ ;; 1200]]];
   quake = Table[ifun[t], {t, 1, 1200, 1}];
   cwd = ContinuousWaveletTransform[quake,
     GaborWavelet[]];
   img = Image[WaveletScalogram[cwd, Axes → False,
      ImageSize → 100]];
   Return[img];
  ];

(* transform the x3b and x3c records into graphical
 representation *)
x4a = ParallelTable[WSgram[x1a[[x3b[[n, 1]]]]],
   {n, 1, x3a}];
x4b = ParallelTable[WSgram[x1a[[x3c[[n, 1]]]]],
   {n, 1, x3a}];
x4c = Table[ImageData[x4a[[n]]][[ ;; , ;; , 1]],
   {n, 1, x3a}];
x4d = Table[ImageData[x4b[[n]]][[ ;; , ;; , 1]],
   {n, 1, x3a}];

(* construct the correlation matrix according to
 ranked graphical representation *)
x5a = Dimensions[x4c[[1]]][[1]];
x5b = Dimensions[x4c[[1]]][[2]];
x5c =
  Table[Abs[Sum[x4c[[i]][[r, c]], {i, 1, x3a}] / x3a -
     Sum[x4d[[i]][[r, c]], {i, 1, x3a}] / x3a],
   {r, 1, x5a}, {c, 1, x5b}];
```

```
(* reduce the correlation matrix to the 0.995
 Quantile of dominant elements and assign weights
 to such elements *)
sparsQ[matrix_] := Module[{i, a, m, pr, pc, l, lf, lfp},
   i = 1;
   a = matrix;
   l = {};
   m = ConstantArray[0,
     {Dimensions[a][[1]], Dimensions[a][[2]]}];
   While[RankedMax[Flatten@a, i] ≥
     Quantile[Flatten@a, 0.995], {i++;
    }];
   For[n = 1, n <= i, n++, {
      l = Append[l, Position[a, RankedMax[Flatten@a, n]]];
     };];
   lf = Flatten@l;
   lfp = Partition[lf, 2];
   For[n = 1, n ≤ Length[lfp], n++, {
     pr = lfp[[n]][[1]];
     pc = lfp[[n]][[2]];
     m[[pr, pc]] = Length[lfp] - (0.99 * n);
    }];
   Return[{m, i}]
  ];
x5d = sparsQ[x5c];

(* transform all records from the full set to
 wavelet scalogram image data *)
x6a = ParallelTable[ImageData[WSgram[x1a[[n]]]][[
     ;; , ;; , 1]], {n, 1, x1b}];
```

```
(* quantify the importance for each record from
 the full set as a product of the reduced
 correlation matrix and the respective image data
 matrix *)
x6b = ParallelTable[Total[Flatten[x5d[[1]] * x6a[[n]]]],
   {n, 1, x1b}];

(* rank the x6b importance vector,
store the respective positions in the full set
 and obtain the responses for the few lowest
 records according to the confidence parameter
 by solving the mechanical model  *)
x7a =
 Table[{RankedMin[x6b, n],
   Position[x6b, RankedMin[x6b, n]],
   Max[
    Abs[
     SDOFxCDM[
      x1a[[
       First@Flatten@Position[x6b,
          RankedMin[x6b, n]]]]]]]}, {n, 1, m}]


(* search for the maximum response within the m
 ranked solved importance vector and consider
 this record critical with respect to selected
 response quantity, such as peak acceleration *)
x8a = Max[10^5 x7a[[ ;; , 3]]]

(*-- end of identification run test case -----------*)



In[7]:= SetOptions[$FrontEnd,
 PrintingStyleEnvironment → "Working"]
```